Evolutionary engineering reveals amino acid substitutions in Ato2 and Ato3 that allow improved growth of Saccharomyces cerevisiae on lactic acid

Baldi, Nicolò; de Valk, Sophie Claire; Sousa-Silva, Maria; Casal, Margarida; Soares-Silva, Isabel; Mans, Robert

DOI
10.1093/femsyr/foab033

Publication date
2021

Document Version
Accepted author manuscript

Published in
FEMS Yeast Research

Citation (APA)
Baldi, N., de Valk, S. C., Sousa-Silva, M., Casal, M., Soares-Silva, I., & Mans, R. (2021). Evolutionary engineering reveals amino acid substitutions in Ato2 and Ato3 that allow improved growth of Saccharomyces cerevisiae on lactic acid. *FEMS Yeast Research*, *21*(4), Article foab033. https://doi.org/10.1093/femsyr/foab033

Evolutionary engineering reveals amino acid substitutions in Ato2 and Ato3 that allow improved growth of *Saccharomyces cerevisia*e on lactic acid**.**

Nicolò Baldi[1]*, Sophie Claire de Valk[1]*, Maria Sousa-Silva[2,3], Margarida Casal[2,3], Isabel Soares-Silva[2,3] & Robert Mans[1]

[1]Department of Biotechnology, Delft University of Technology, Van der Maasweg 9, 2629HZ Delft, The Netherlands

[2]Centre of Molecular and Environmental Biology (CBMA), University of Minho, Campus de Gualtar, Braga, Portugal

[3]Institute of Science and Innovation for Bio-Sustainability (IB-S), University of Minho, Campus de Gualtar, Braga, Portugal

*Shared-first authorship

Corresponding author: Robert Mans, r.mans@tudelft.nl

Running title: Novel lactic acid transporters in yeast.

Manuscript for submission to FEMSYR

ABSTRACT

In *Saccharomyces cerevisiae*, the complete set of proteins involved in transport of lactic acid across the cell membrane has not been determined. In this study we aimed to identify transport proteins not previously described to be involved in lactic acid transport via a combination of directed evolution, whole-genome resequencing and reverse engineering. Evolution of a strain lacking all known lactic acid transporters on lactate led to the discovery of mutated Ato2 and Ato3 as two novel lactic acid transport proteins. When compared to previously identified *S. cerevisiae* genes involved in lactic acid transport, expression of $ATO3^{T284C}$ was able to facilitate the highest growth rate (0.15 ± 0.01 h^{-1}) on this carbon source. A comparison between (evolved) sequences and 3D models of the transport proteins showed that most of the identified mutations resulted in a widening of the narrowest hydrophobic constriction of the anion channel. We hypothesize that this observation, sometimes in combination with an increased binding affinity of lactic acid to the sites adjacent to this constriction, are responsible for the improved lactic acid transport in the evolved proteins.

1. INTRODUCTION

The yeast *Saccharomyces cerevisiae* is able to utilize a variety of compounds as carbon and energy source, including monosaccharides, disaccharides, monocarboxylic acids, amino acids and polyols (Kruckeberg and Dickinson, 2004; Lagunas, 1993). Assimilation and dissimilation of these compounds inside cells is preceded by their transport across the plasma membrane. A lot of research has been dedicated to the identification of proteins involved in the uptake and the elucidation of their structure, function and mechanism of action, both to understand cellular response to different conditions as well as for the application of metabolic engineering strategies to increase the efficiency of substrate usage and broaden the substrate range of industrial cell factories (Agrimi and Steiger, 2021).

This research field has tremendously benefitted from engineered 'platform strains', in which all transporters for a certain substrate have been knocked out. One of the most applied platform strains is the so called '*hxt*^{0} strain', in which the uptake of hexoses is completely abolished by the knockout of all 21 genes involved in uptake of hexoses (Wieczorke et al., 1999). This *hxt*^{0} strain has been indispensable for studies where both endogenous and heterologous proteins were characterized for their ability to catalyze the uptake of various hexose and pentose sugars (Anjos et al., 2013; Bueno et al., 2020; Chattopadhyay et al., 2020; Gao et al., 2019; Huang et al., 2020; Li et al., 2015; Morii et al., 2020). The absence of all hexose transporters in this strain renders it unable to grow on media in which a monosaccharide is the sole carbon source, and therefore allows for screening of growth phenotypes that are linked to the expression of an investigated transport protein. The application of the *hxt*^{0} strain is also preferred for *in vivo* transport assays in which the intracellular accumulation of substrates is measured, since background signal caused by other transporters is minimized (Nogueira et al., 2020; Paulsen et al., 2019; Schmidl et al., 2021). In addition, it has often

been used as background strain in directed evolution of (heterologous) transport proteins, for which selection is based on growth on the transported substrate (Colabardini et al., 2014; Li et al., 2016; Nijland and Driessen, 2020; Sloothaak et al., 2016; Wang et al., 2013; Zhang et al., 2015). The benefit of a platform strain in an evolutionary engineering approach is that the presence of other genes that could (upon mutation) provide a selective advantage is minimized, and thus allows for improved selection of mutants of the gene under investigation. Similar platform strains have been constructed to study disaccharide transporters (Riesmeier et al., 1992) and ABC transporters (Suzuki et al., 2011).

Transport of monocarboxylic acids across the yeast plasma membrane remains enigmatic (Borodina, 2019) and therefore the establishment of specialized platform strains to study transport of specific monocarboxylic acids could be an important next step to further our understanding. Whereas the undissociated, protonated form of carboxylic acids can cross biological membranes by passive diffusion, the charged anionic form that is predominant in pH conditions well above the pK_a of the acid requires (a) protein(s) to mediate rapid transport across the membrane (Gabba et al., 2020). These monocarboxylic acid transport proteins play an important role in, for instance, food preservation, weak organic acid tolerance in second generation bioethanol production, metabolic engineering strategies for industrial production of carboxylic acids and in development of cancer therapies (Pinheiro et al., 2012; Soares-Silva et al., 2020). Two genes encoding permeases for monocarboxylic acids have been identified so far in *S. cerevisiae*: *JEN1* and *ADY2* (Casal et al., 2016). Jen1 is a member of the Major Facilitator Superfamily which enables uptake of lactic, acetic and pyruvic acid (Casal et al., 1999). Ady2 is an acetate transporter that belongs to the AceTr family, for which two homologs have been described in *S. cerevisiae*, Ato2 and Ato3 (Paiva et al., 2004; Ribas et al., 2019). A powerful strategy to identify more genes involved in a specific physiological

function is the use of adaptive laboratory evolution. Application of a selective pressure is used to enrich for mutants with the phenotype of interest, which can subsequently be analyzed by whole genome sequencing to identify mutated genes related to the evolved phenotype (Mans et al., 2018). This concept was demonstrated in a previous study, in which laboratory evolution of a *jen1Δ* strain in culture medium with lactic acid as sole carbon source led to the identification of mutated *ADY2* alleles that had an increased uptake capacity for lactic acid (de Kok et al., 2012). Lactic acid, which is produced on industrial scale using biotechnological processes, is used as preservative in the dairy industry and as a precursor for the production of bioplastic, with a demand of 1.220.000 tons in 2016 that is expected to further increase by 16.2% before 2025 (Singhvi et al., 2018).

In this study, we use adaptive laboratory evolution to identify additional transporters, which upon mutation can efficiently catalyze lactic acid uptake in *S. cerevisiae*. Subsequently, we overexpress the complete suite of native and evolved lactic acid transporters in a strain background devoid of all (putative) organic acid transporters, characterize the ability of the resulting strains to grow on monocarboxylic acids and assess the uptake of labelled lactate and acetate by the evolved transporters. Finally, we identify specific amino acid residues playing a key role in the transport of lactic acid and provide a mechanistic explanation using three-dimensional structure predictions combined with molecular docking analysis.

2. MATERIALS AND METHODS

2.1 Strains and maintenance

The *S. cerevisiae* strains used in this study (Table 2) share the CEN.PK113-7D or the CEN.PK2-1C genetic backgrounds (Entian and Kötter, 2007). Stock cultures of *S. cerevisiae* were grown aerobically in 500 mL round-bottom shake flasks containing 100 mL synthetic medium (SM) (Verduyn et al., 1992) or YP medium (10 g L^{-1} Bacto yeast extract, 20 g L^{-1} Bacto peptone) supplemented with 20 g L^{-1} glucose. When needed, auxotrophic requirements were complemented via addition of 150 mg L^{-1} uracil, 100 mg L^{-1} histidine, 500 mg L^{-1} leucine and/or 75 mg L^{-1} tryptophan (Pronk, 2002). For plate cultivation, 2% (w/v) agar was added to the medium prior to heat sterilization. Stock cultures of *E. coli* XL1-Blue Subcloning Grade Competent Cells (Agilent, Santa Clara, CA, USA) that were used for plasmid propagation were grown in LB medium (5 g L^{-1} Bacto yeast extract, 10 g L^{-1} Bacto tryptone, 10 g L^{-1} NaCl) supplemented with 100 mg L^{-1} ampicillin. Media were autoclaved at 121°C for 20 min and supplements and antibiotics were filter sterilized and added to the media prior to use. Frozen culture stocks were prepared by addition of sterile glycerol (to a final concentration of 30% v/v) to exponentially growing shake flask cultures of *S. cerevisiae* or overnight cultures of *E. coli* and 1 mL aliquots were stored at -80°C.

2.2 Molecular biology techniques

Phusion High-Fidelity DNA Polymerase (Thermo Fisher Scientific, Waltham, MA, USA) was used for PCR amplification for cloning purposes. Diagnostic PCRs were performed using DreamTaq PCR Master Mix (2X) (Thermo Fisher Scientific). In both cases, the manufacturer's protocol was followed, with the exception of the use of lower primer concentrations (0.2 µM each). Desalted (DST) oligonucleotide primers were used, except for primers binding to coding regions, which were PAGE purified. Primers were purchased from Sigma Aldrich (Saint Louis,

MO, USA), with the exception of primers 17453 and 17453, which were purchased from Ella Biotech (Planegg, Germany). For diagnostic PCR, yeast genomic DNA was isolated as described by (Lõoke et al., 2011). Commercial kits for DNA extraction and purification were used for small-scale DNA isolation (Sigma Aldrich), PCR cleanup (Sigma Aldrich), and gel extraction (Zymo Research, Irvine, CA, USA). Restriction analysis of constructed plasmids was performed using FastDigest restriction enzymes (Thermo Scientific). Gibson assembly of linear DNA fragments was performed using NEBuilder HiFi DNA Assembly Master Mix (New England Biolabs, Ipswich, MA, USA) in a total reaction volume of 5 µL. Transformation of chemically competent *E. coli* XL1-Blue (Agilent) was performed according to the manufacturer's protocol.

2.3 Plasmid construction

The plasmids and oligonucleotide primers used in this study are listed in Table 1 and Supplementary Table 1, respectively. All plasmids were constructed by Gibson assembly of two linear fragments. With the exception of the fragments used for the construction of plasmid pUDR420, all fragments were PCR-amplified from either a template plasmid or from genomic DNA.

Plasmid pUDR405 was constructed by Gibson assembly of two linear fragments, both obtained via PCR amplification of plasmid pROS13 using primers 8664 and 6262 (for the *JEN1*-gRNA_2µ_*ADY2*-gRNA insert) and 6005 (for the plasmid backbone), as previously described by (Mans et al., 2015). Plasmid pUDR420 was constructed by Gibson assembly of a double-stranded DNA fragment, obtained by annealing the complementary single-stranded oligonucleotides 8691 and 13552, and a vector backbone amplified from plasmid pMEL13 using primers 6005 and 6006. Plasmid pUDR767 was constructed by Gibson assembly of two linear fragments, both obtained via PCR amplification of plasmid pROS10 using primers 8688

(for the *ATO2*-gRNA_2µ_*ATO2*-gRNA insert) and 6005 (for the plasmid backbone). For construction of pUDE813, the linear p426-TEF plasmid backbone was amplified from plasmid p426-TEF using primers 5921 and 10547 and the *ATO3* open reading frame (ORF) was amplified from yeast strain CEN.PK113-7D genomic DNA using primers 13513 and 13514. Subsequently, Gibson assembly of the linear p426-TEF plasmid backbone and the *ATO3* insert yielded pUDE813. pUDE814, pUDE1001, pUDE1002, pUDE1003, pUDE1004, pUDE1021 and pUDE1022 were constructed similar to pUDE813, using primers 5921 and 10547 to amplify the linear p427-TEF plasmid backbone. The inserts were amplified from genomic DNA of strain CEN.PK113-7D (for wildtype genes) or from genomic DNA of the corresponding evolved strain (for mutated genes) using primers 13513 and 13514 (pUDE814), 17170 and 17171 (pUDE1001), 17168 and 17169 (pUDE1002, pUDE1003 and pUDE1004) or 17452 and 17453 (pUDE1021 and pUDE1022). For construction of pUDC319, plasmid p426-TEF was amplified using primers 2949 and 17741 and the CEN6 origin of replication was amplified from pUDC156 using primers 17742 and 17743. Subsequently, Gibson assembly of the linear p426-TEF plasmid fragment and the CEN6 fragment yielded pUDC319. pUDC320, pUDC321, pUDC322, pUDC323, pUDC324, pUDC325, pUDC326 and pUDC327 were constructed in a similar way using the same primers, but the linear plasmid fragment was amplified from pUDE813, pUDE814, pUDE1001, pUDE1002, pUDE1003, pUDE1004, pUDE1021 and pUDE1022, respectively.

Table 1: Plasmids used in this study.

Name	**Relevant characteristic**	**Origin**
pROS13	2µm ampR *kanMX* gRNA-*CAN1* gRNA-	(Mans et al., 2015)

	ADE2	
pROS10	2*µ*m ampR *URA3* gRNA-*CAN1* gRNA-*ADE2*	(Mans et al., 2015)
pMEL13	2*µ*m ampR *kanMX* gRNA-*CAN1*	(Mans et al., 2015)
pUDR405	2*µ*m ampR *kan*MX gRNA-*JEN1* gRNA-*ADY2*	This study
pUDR420	*2µm ampR kanMX gRNA-ATO3*	This study
pUDR767	2*µ*m ampR *URA3* gRNA-*ATO2*	This study
p426-TEF	2*µ*m *URA3 pTEF1-tCYC1*	(Mumberg et al., 1995)
pUDE813	2*µ*m *URA3 pTEF1-ATO3-tCYC1*	This study
pUDE814	*2µm URA3 pTEF1-ATO3^{T284C}-tCYC1*	This study
pUDE1001	2*µ*m *URA3 pTEF1-JEN1-tCYC1*	This study
pUDE1002	2*µ*m *URA3 pTEF1-ADY2-tCYC1*	This study
pUDE1003	*2µm URA3 pTEF1- ADY2^{C755G} -tCYC1*	This study
pUDE1004	*2µm URA3 pTEF1- ADY2^{C655G}-tCYC1*	This study
pUDE1021	2*µ*m *URA3 pTEF1-ATO2-tCYC1*	This study
pUDE1022	*2µm URA3 pTEF1-ATO2^{T653C}-tCYC1*	This study
pUDC156	*CEN6 URA3 pTEF-CAS9-tCYC1*	(Marques et al., 2017)
pUDC319	*CEN6 URA3 pTEF-tCYC1*	This study
pUDC320	*CEN6 URA3 pTEF1-ATO3-tCYC1*	This study
pUDC321	*CEN6 URA3 pTEF1-ATO3^{T284C}-tCYC1*	This study
pUDC322	*CEN6 URA3 pTEF1-JEN1-tCYC1*	This study
pUDC323	*CEN6 URA3 pTEF1-ADY2-tCYC1*	This study
pUDC324	*CEN6 URA3 pTEF1- ADY2^{C755G} -tCYC1*	This study
pUDC325	*CEN6 URA3 pTEF1- ADY2^{C655G}-tCYC1*	This study
pUDC326	*CEN6 URA3 pTEF1-ATO2-tCYC1*	This study
pUDC327	*CEN6 URA3 pTEF1-ATO2^{T653C}-tCYC1*	This study

171

172

2.4 Strain construction

S. cerevisiae strains were transformed with the LiAc/ssDNA method (Gietz and Woods, 2002). For transformations with a dominant marker, the transformation mixture was plated on YP plates, containing glucose (20 g L^{-1}) as carbon source, and supplemented with 200 mg L^{-1} G418 (Invitrogen, Carlsbad, CA, USA). Gene deletions were performed as previously described (Mans et al., 2015). For transformation of plasmids harboring an auxotrophic marker, transformed cells were plated on SM medium with glucose (20 g L^{-1}) as a carbon source and when needed, appropriate auxotrophic requirements were supplemented.

The tryptophan auxotrophy of IMX1000 was the result of a single point mutation in the *TRP1* gene (*trp1-289*) (Botstein et al., 1979) and was spontaneously reverted by plating the strain on SM medium supplemented with uracil, histidine and leucine, and picking a tryptophan prototrophic colony, yielding strain IMX2486. Strain IMX2487 was constructed by transforming IMX2486 with a linear fragment, obtained by PCR amplification of the *LEU2* gene from CEN.PK113-7D, using primers 1742 and 1743. Strain IMX2488 was constructed by transforming IMX2487 with a linear fragment, obtained by PCR amplification of the *HIS3* gene from CEN.PK113-7D, using primers 1738 and 3755. Strain IMK875 was constructed by transforming the Cas9-expressing strain IMX585 with plasmid pUDR405 and two double stranded repair oligonucleotides obtained by annealing oligonucleotides 8597 to 8598 and 8665 to 8666. Strain IMK876 was constructed by transforming the Cas9-expressing strain IMX581 with plasmid pUDR405 and two double stranded repair oligonucleotides obtained by annealing oligonucleotides 8597 to 8598 and 8665 to 8666. Strains IMK882 and IMK883 were obtained by transforming strains IMK875 and IMK876, respectively, with plasmid pUDR420 and a double stranded repair oligonucleotide obtained by annealing oligonucleotides 14120

196 and 14121. Strain IMK982 was constructed by transforming strain IMK883 with plasmid
197 pUDR767 and a double stranded repair oligonucleotide obtained by annealing
198 oligonucleotides 8689 and 8690. Plasmids p426-TEF, pUDE813, pUDE814, pUDE1001,
199 pUDE1002, pUDE1003, pUDE1004, pUDE1021, pUDE1022, pUDC319, pUDC320, pUDC321,
200 pUDC322, pUDC323, pUDC324, pUDC325, pUDC326 and pUDC327 were transformed in strain
201 IMX2488, yielding IME581, IME582, IME583, IME584, IME585, IME586, IME587, IME588,
202 IME589, IMC164, IMC165, IMC166, IMC167, IMC168, IMC169, IMC170, IMC171 and IMC172,
203 respectively.

204 Evolution of IMK341 and IMK882 was performed by inoculating duplicate shake flasks
205 with 20 mL synthetic medium with lactic acid as the sole carbon source (SML, see section 2.5
206 'Media and cultivation') with these strains to obtain a starting optical density (OD) of 0.1. Once
207 the cultures grew and stationary phase was reached, a 1 mL aliquot of each culture was
208 transferred to 20 ml fresh SML and grown until stationary phase again (in total approximately
209 14 generations for IMK341 and 7 generations for IMK882). Single colony isolates from these
210 evolution cultures ('IMS'-strains) were obtained by plating the cultures using an inoculation
211 loop (~10 µl) on solid SML and restreaking a grown colony to a fresh plate three consecutive
212 times, after which one colony was grown in liquid SML and stocked.

213 Table 2: *Saccharomyces cerevisiae* strains used in this study

Strain name	Relevant genotype [a]	Origin
CEN.PK113-7D	Prototrophic reference, *MAT*a	(Entian and Kötter, 2007)
IMX581	*MAT*a *ura3-52 can1::cas9-natNT2*	(Mans et al., 2015)
IMX585	*MATa can1::cas9-natNT2*	(Mans et al., 2015)
IMK341	*MATa ura3::loxP ady2::loxP-hphNT1-*	(de Kok et al.,

	loxP jen1::loxP	2012)
IMW004	*MATa URA3 ADY2^{C755G} jen1::loxP-KanMX4-loxP*	(de Kok et al., 2012)
IMW005	*MATa URA3 ADY2^{C655G} jen1::loxP-KanMX4-loxP*	(de Kok et al., 2012)
IMX1000	*MATa ura3-52 trp1-289 leu2-3112 his3Δ can1Δ::cas9-natNT2 mch1Δ mch2Δ mch5Δ aqy1Δ itr1Δ pdr12Δ mch3Δ mch4Δ yil166cΔ hxt1Δ jen1Δ ady2Δ aqr1Δ thi73Δ fps1Δ aqy2Δ yll053cΔ ato2Δ ato3Δ aqy3Δ tpo2Δ yro2Δ azr1Δ yhl008cΔ tpo3Δ*	(Mans et al., 2017)
IMK875	*MATa can1::cas9-natNT2 jen1Δ ady2Δ*	This study
IMK876	*MATa can1::cas9-natNT2 ura3-52 jen1Δ ady2Δ*	This study
IMK882	*MATa can1::cas9-natNT2 jen1Δ ady2Δ ato3Δ*	This study
IMK883	*MATa can1::cas9-natNT2 ura3-52 jen1Δ ady2Δ ato3Δ*	This study
IMK982	*MATa can1::cas9-natNT2 ura3-52 jen1Δ ady2Δ ato3Δ ato2Δ*	This study
IMS807	IMK341 evolved for growth on lactate, evolution line A	This study
IMS808	IMK341 evolved for growth on lactate, evolution line A	This study
IMS809	IMK341 evolved for growth on lactate, evolution line A	This study
IMS810	IMK341 evolved for growth on lactate, evolution line B	This study
IMS811	IMK341 evolved for growth on lactate, evolution line B	This study
IMS1122	IMK882 evolved for growth on lactate	This study
IMS1123	IMK882 evolved for growth on lactate	This study
IMS1130	IMK882 evolved for growth on lactate	This study
IMX2486	IMX1000 *ura3-52 TRP1, leu2-3112,*	This study

	his3Δ	
IMX2487	IMX1000 *ura3-52 TRP1*, *LEU2*, *his3Δ*	This study
IMX2488	IMX1000 *ura3-52 TRP1*, *LEU2*, *HIS3*	This study
IME581	IMX2488 p426-TEF (2*μ*m)	This study
IME582	IMX2488 pUDE813 (2*μ*m *ATO3*)	This study
IME583	IMX2488 pUDE814 (2*μ*m $ATO3^{T284C}$)	This study
IME584	IMX2488 pUDE1001 (2*μ*m *JEN1*)	This study
IME585	IMX2488 pUDE1002 (2*μ*m *ADY2*)	This study
IME586	IMX2488 pUDE1003 (2*μ*m $ADY2^{C755G}$)	This study
IME587	IMX2488 pUDE1004 (2*μ*m $ADY2^{C655G}$)	This study
IME588	IMX2488 pUDE1021 (2*μ*m *ATO2*)	This study
IME589	IMX2488 pUDE1022 (2*μ*m $ATO2^{T653C}$)	This study
IMC164	IMX2488 pUDC319 (*CEN6*)	This study
IMC165	IMX2488 pUDC320 (*CEN6 ATO3*)	This study
IMC166	IMX2488 pUDC321 (*CEN6* $ATO3^{T284C}$)	This study
IMC167	IMX2488 pUDC322 (*CEN6 JEN1*)	This study
IMC168	IMX2488 pUDC323 (*CEN6 ADY2*)	This study
IMC169	IMX2488 pUDC324 (*CEN6* $ADY2^{C755G}$)	This study
IMC170	IMX2488 pUDC325 (*CEN6* $ADY2^{C655G}$)	This study
IMC171	IMX2488 pUDC326 (*CEN6 ATO2*)	This study
IMC172	IMX2488 pUDC327 (*CEN6* $ATO2^{T653C}$)	This study

2.5 Media and cultivation

Evolution experiments were performed in 500 mL shake-flask cultures containing 100 mL synthetic medium (Verduyn et al., 1992) with 84 mM L-lactic acid as sole carbon source. The pH of the medium was set at 5.0 and the cultures were incubated at 30°C in an Innova incubator shaker (New Brunswick Scientific, Edison, NJ, USA) set at 200 rpm. Auxotrophic requirements were supplemented as needed.

Strains were characterized in SM supplemented with different carbon sources. To achieve an initial carbon concentration of 250 mM, the culture media contained either 42 mM

D-glucose, 83 mM L-lactic acid, 125 mM acetic acid or 83 mM pyruvic acid. The characterization was performed in a Growth-Profiler system (EnzyScreen, Heemstede, The Netherlands) equipped with 96-well plates in a culture volume of 250 µL, set at 250 rpm and 30°C. The measurement interval was set at 30 minutes. Raw green values were corrected for well-to-well variation using measurements of a 96-well plate containing a culture with an externally determined optical density of 3.75 in all wells. Optical densities were calculated by converting green values (corrected for well-to-well variation) using a calibration curve that was determined by fitting a third-degree polynomial through 22 measurements of cultures with known OD values between 0.1 and 20. Growth rates were calculated using the calculated optical densities of at least 15 points in the exponential phase. Exponential growth was assumed when an exponential curve could be fitted with an R^2 of at least 0.985.

2.6 Analytical methods

Culture optical density at 660 nm was measured with a Libra S11 spectrophotometer (Biochrom, Cambridge, United Kingdom). In order to measure within the linear range of the instrument (OD between 0.1 and 0.3), cultures were diluted in an appropriate amount of demineralized water. Metabolite concentrations in culture supernatants and media were analyzed using an Agilent 1260 Infinity HPLC system equipped with a Bio-rad Aminex HPX-87H ion exchange column, operated at 60°C with 5 mM H_2SO_4 as mobile phase at a flow rate of 0.600 mL min^{-1}.

2.7 DNA extraction and whole genome sequencing

Strain IMK341 and the evolved single colony isolates (IMS-strains) were grown in 500 mL shake flasks containing 100 mL YP medium supplemented with glucose (20 g L^{-1}) as a carbon source. The cultures were incubated at 30°C until the strains reached stationary phase and genomic

DNA was isolated using the Qiagen 100/G kit (Qiagen, Hilden, Germany) according to the manufacturer's instructions and quantified using a Qubit® Fluorometer 2.0 (Thermo Fisher Scientific). The isolated DNA was sequenced in-house on a MiSeq (Illumina, San Diego, CA, USA) with 300 bp paired-end reads using TruSeq PCR-free library preparation (Illumina). For all the strains, the reads were mapped onto the *S. cerevisiae* CEN.PK113-7D genome (Salazar et al., 2017) using the Burrows–Wheeler Alignment tool (BWA) and further processed using SAMtools and Pilon for variant calling (Li and Durbin, 2010; Li et al., 2009; Walker et al., 2014).

2.8 Transport assays

The uptake of labelled carboxylic acids was assessed as previously described by (Ribas et al., 2017), using [1-^{14}C] acetic acid (Perkin Elmer, Massachusetts, USA) and [U-^{14}C] L-lactic acid (Perkin Helmer, Massachusetts, USA) with a specific activity of 2000 dpm/nmol. The data shown are mean values of at least three independent experiments.

2.9 3D modelling and molecular docking of Ady2, Ato2 and Ato3

The three-dimensional modelling analysis was performed for the protein sequences of Ato1, Ady2^{L219V}, Ady2^{A252G}, Ato2, Ato2^{L218S}, Ato3 and Ato3^{F95S}. The amino acid sequences were retrieved from the *Saccharomyces* Genome Database (Cherry et al., 2012). To determine the predicted transporter 3D structures, the amino acid sequences were threaded through the PDB library using LOMETS (Local Meta-Threading-Server). The *Citrobacter koseri* succinate acetate permease (CkSatP, PDB 5YS3) was the top ranked template threading identified in LOMETS for Ato1, Ato2 and Ato3 (Qui et al., 2018). Since the CkSatP three-dimensional modelling obtained the best score for protein structure prediction, it was further considered for molecular docking analysis. CkSatP presents a protein identity of 35% with Ady2, 34% with Ato2 and 28% with Ato3 and similarity of 0.566, 0.548 and 0.515, respectively. Molecular

docking simulations were performed as described by (Ribas et al., 2017). Ligand structures of acetic, lactic and pyruvic acid for all target proteins in the study were downloaded from the Zinc database (Sterling and Irwin, 2015). Structures used for docking were all confirmed in Maestro v11.2 before ligand-protein simulations were performed using AutoDock Vina in the PyRx software (Trott and Olson, 2010). The docking studies were performed with the dissociated forms of each carboxylic acid. The protonation states were adjusted to match a pH of 5.0-6.0 and exported in the mol2 format. Docking was performed with four docking-boxes for each protein, containing top, bottom and middle-structure parts for a more robust use of Autodock Vina program. The exhaustiveness parameter was set up for 1000 calculations for each of the grid-zones defined for docking. The generated docking scores and 2-3D pose views were evaluated for the establishment of molecular interactions and ligand binding affinities.

3. RESULTS

3.1 Laboratory evolution on lactic acid leads to point mutations in Ato2 or Ato3

In an attempt to identify additional transporters able to catalyze the uptake of lactic acid after gaining point mutations, we incubated strains IMK341 and IMX1000 in duplicate shake flasks cultures containing synthetic medium with lactic acid as the sole carbon source. In IMK341 the known carboxylic acid transporters *JEN1* and *ADY2* are knocked out (*jen1Δ*, *ady2Δ*), whereas IMX1000 contains a further 23 deletions in putative lactic acid transporter-encoding genes (Table 2) (Mans et al., 2017). After 9 weeks, growth was observed in both cultures of IMK341 whereas no growth was observed after 12 weeks of incubation of IMX1000. Whole-genome sequencing of evolved IMK341 (*jen1Δ*, *ady2Δ*) cell lines, named IMS807-811 which were isolated after a transfer to fresh medium, revealed three to seven non-synonymous SNPs in each mutant and no chromosomal duplications or rearrangements (Table 3). Strikingly, all evolved isolates shared an identical mutation in *ATO3* (*ATO3*^{T284C}). To investigate the role of *ATO3* in lactic acid uptake, we overexpressed both the native and evolved *ATO3* in IMK883 (*jen1Δ*, *ady2Δ*, *ato3Δ*) and tested the resulting strains for growth on SM lactic acid plates. After 5 days, only the reference strain CEN.PK113-7D and the strain carrying the *ATO3*^{T284C} allele were able to grow (Supplementary Figure 1), indicating that the T284C mutation in *ATO3* was responsible for the evolved phenotype. We then combined the deletion of *JEN1*, *ADY2* and *ATO3* in strain IMK882 (*jen1Δ, ady2Δ, ato3Δ*) and repeated the evolution. After 5 and 12 days, growth was observed in two independent cultures from which evolved strains IMS1122 and IMS1123 were isolated after transfer to a flask with fresh medium. In both single colony isolates, five SNPs were present (Table 3), including a common mutation in *ATO2*, (*ATO2*^{T653C}), which has also been described as an ammonium transporter together with *ATO3* and *ADY2*

(Palková et al., 2002). Finally, the evolution was repeated with IMK982 (*jen1Δ, ady2Δ, ato3Δ, ato2Δ)*, but no growth was observed after 12 weeks of incubation.

Table 3: Amino acid changes identified by whole-genome sequencing of single colony isolates evolved for growth in medium containing lactic acid as sole carbon source. Isolates IMS807 to IMS811 are derived from IMK341 (*jen1Δ*, *ady2Δ*) and IMS1122 and IMS1123 are derived from IMK882 (*jen1Δ*, *ady2Δ*, *ato3Δ*)). IMS807, IM808 and IMS809 are isolates from evolution line #1 and IMS810 and IMS811 are isolates from evolution line #2. The mutation Sip5^{*490Q} indicates loss of the stop codon.

IMK341 evolution #1			IMK341 evolution #2		IMK822 evolution #1	IMK822 evolution #2
IMS807	IMS808	IMS809	IMS810	IMS811	IMS1122	IMS1123
Ato3^{F95S}	**Ato3^{F95S}**	**Ato3^{F95S}**	**Ato3^{F95S}**	**Ato3^{F95S}**	**Ato2^{L218S}**	**Ato2^{L218S}**
Mms2^{Y58C}	Mms2^{Y58C}	Mms2^{Y58C}	Sip5^{*490Q}	Sip5^{*490Q}	Lrg1^{H979N}	Whi2^{E119*}
Pih1^{D147Y}	Pih1^{D147Y}	Pih1^{D147Y}	Ssn2^{M1280R}	Lip5^{R4L}	Ykr051w^{Y285H}	Ykr051w^{Y285H}
Uba1^{L952F}		Drn1^{P213L}			Jjj1^{H356Q}	Jjj1^{H356Q}
Stv1^{L275F}					Trm10^{A49V}	Trm10^{A49V}
Whi2^{E187*}						
Vba4^{P198L}						

3.2 Overexpression of mutated transporters enables rapid growth in liquid medium with lactic acid as sole carbon source

Strikingly, the evolved transporters able to catalyze the uptake of lactic acid (*ATO2* and *ATO3* in this study, and *ADY2* in work by de Kok et al., 2012) represent all members of the *S. cerevisiae* Acetate Uptake Transporter Family (TCDB 2.A.96). To characterize the impact of the mutations on the transport of organic acids, cellular growth was evaluated in strains individually expressing *JEN1, ADY2, ATO2* and *ATO3* and their mutated alleles under control of the strong *TEF1* promotor (Mumberg et al., 1995), via centromeric vectors in IMX2488, a strain background in which 25 (putative) organic acid transporters were deleted (Table 2). No viable cultures could be obtained with strains overexpressing wildtype *ATO2*, which suggests a severe toxic effect of the overexpression of *ATO2* on cellular physiology, and for this reason

no growth rate could be reported. All other IMX2488-derived transporter expressing strains had similar growth rates in liquid medium with 42 mM glucose as carbon source compared to the empty vector control (IMC164), indicating no major physiological effects caused by the overexpression of the transporters when grown on glucose (Figure 1, top left panel). Overexpression of the transporter variants from multicopy vectors resulted in a growth rate reduction of up to 66% compared to the empty vector reference when grown on glucose and were therefore not tested further (Supplementary Figure 2). In accordance with previous research, strains overexpressing *ADY2*, *ADY2*^{C755G} and *ADY2*^{C655G} showed a maximum specific growth rate of 0.02 ± 0.01 h^{-1}, 0.08 ± 0.01 h^{-1} and 0.10 ± 0.01 h^{-1} when grown in medium containing 83 mM lactic acid as carbon source, respectively (de Kok et al., 2012). Surprisingly, strains expressing the evolved *ATO2*^{T653C} and *ATO3*^{T284C} alleles outperformed all the other tested strains, with maximum specific growth rates of 0.11 ± 0.01 h^{-1} and 0.15 ± 0.01 h^{-1}, respectively (Figure 1, top right panel and Supplementary Figure 5). These represent the highest reported growth rates reported for *S. cerevisiae* on this carbon source and indicate that, similar to the role of evolved Ato3 in IMS807-811, the mutations in Ato2 are responsible for the evolved phenotypes observed in IMS1122 and IMS1123 (Table 3). The transport of labelled lactic acid in strains expressing native *ATO3* and evolved *ADY2*, *ATO2* and *ATO3* is in accordance with the observed growth phenotypes (Figure 2). An increased uptake rate was observed for all strains overexpressing evolved transporters compared to the empty vector control strain, whereas expression of wildtype *ATO3* did not lead to a significant alteration in lactic acid uptake (Figure 2).

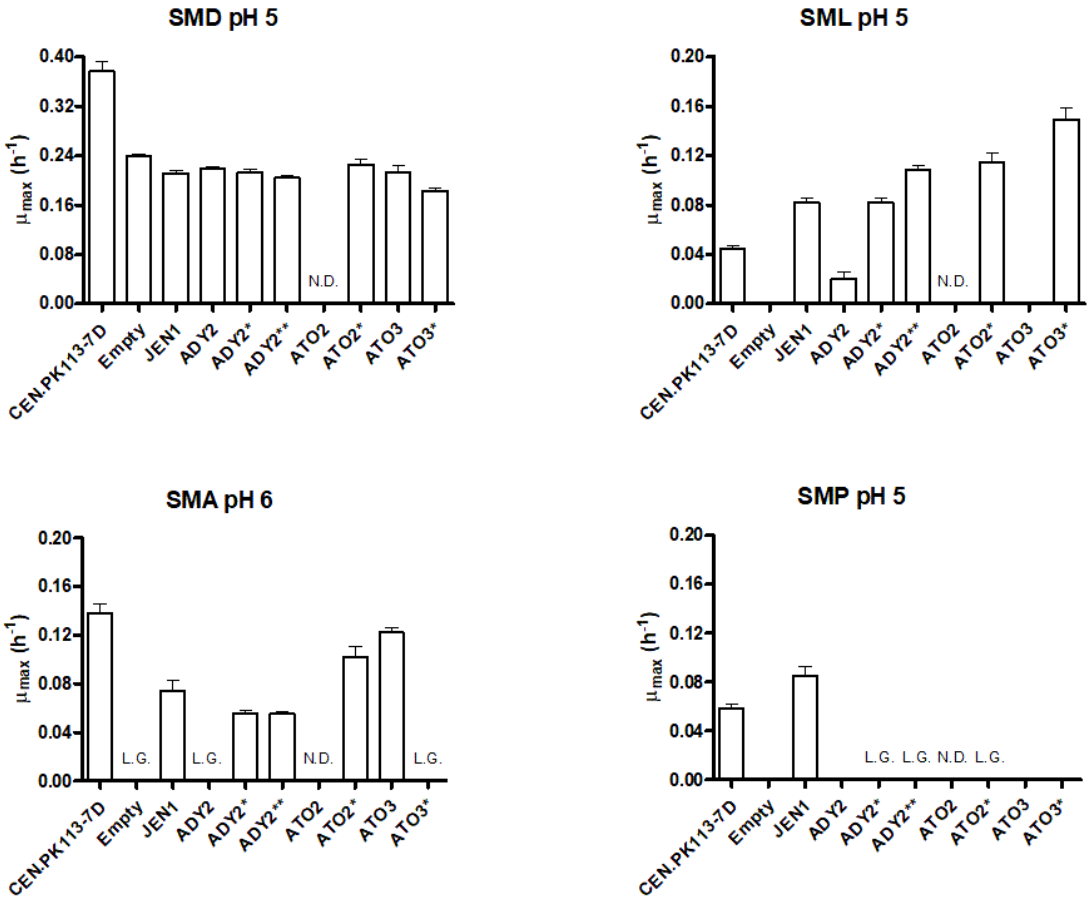

Figure 1: Growth rates on different sole carbon sources of *S. cerevisiae* reference strain CEN.PK113-7D and the 25-transporter deletion strain IMX2488 expressing an empty vector or a vector carrying the indicated organic acid transporter. Bars and error bars represent the average and standard deviation of three independent experiments. SMD: synthetic medium with 42 mM glucose. SML: synthetic medium with 83 mM lactic acid. SMA: synthetic medium with 125 mM acetic acid. SMP: synthetic medium with 83 mM pyruvic acid. Empty: empty plasmid. ADY2*: *ADY2*^{C755G} allele. ADY2**: *ADY2*^{C655G} allele. ATO2*: *ATO2*^{T653C} allele. ATO3*: *ATO3*^{T284C} allele. For some experiments, a linear increase in optical density was observed, which impeded the determination of an exponential growth rate (indicated by L.G. for Linear Growth). N.D.: not determined.

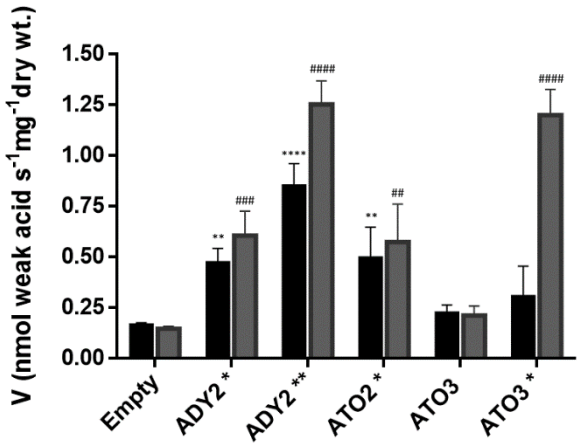

Figure 2: Transport of acetate and lactate in *S. cerevisiae* IMX1000 cells expressing native and evolved *ADY2*, *ATO2* and *ATO3*. Black bars: uptake of 5 mM of ^{14}C-acetic acid (pH 6.0). Grey bars: uptake of ^{14}C-lactic acid (pH 5.0). Empty: empty plasmid. ADY2*: $ADY2^{C755G}$ allele. ADY2**: $ADY2^{C655G}$ allele. ATO2*: $ATO2^{T653C}$ allele. ATO3*: $ATO3^{T284C}$ allele. Cells were grown on YNB-glucose, washed and incubated in YNB-lactate (0.5 %, pH 5.0) for 4 hours at 30°C. Statistical significance was estimated by one-way ANOVA followed by a post hoc Tukey's multiple comparisons test as follows: ** p<0.01, *** p<0.001, **** p<0.0001, acetate uptake significantly different from cells transformed with empty plasmid; ## p<0.01, ### p<0.001, #### p<0.0001, lactate uptake significantly different from cells transformed with empty plasmid.

3.3 Mutations in *ATO2* and *ATO3* alter the uptake capacity for acetate and pyruvate

After demonstrating that the point mutations increased the catalytic activity of Ato2, Ato3 and Ady2 for lactic acid transport, we also investigated their ability to transport acetic and pyruvic acid (Figure 1, bottom panels and Supplementary Figures 6 and 7). In liquid medium at pH 5.0 with 125 mM acetic acid (pK_a of 4.75), no growth was observed for any of the strains with the 25-deletion background, likely caused by acetic acid toxicity due to the absence of essential acetic acid exporters (Supplementary Figure 3). However, at pH 6.0 different growth characteristics were observed. The empty vector control strain exhibited slow non-exponential growth, which was also observed for the strains expressing native *ADY2* and the evolved *ATO3* variant. On the other hand, expression of native *ATO3* and the evolved *ADY2* and *ATO2* variants improved growth performance on medium with acetic acid as sole carbon source. With the exception of native *ATO3*, these results are in accordance with

improved uptake rates observed in these strains, determined with labelled acetate (Figure 2). In medium containing 83 mM pyruvic acid, no exponential growth was observed for any of the strains expressing Ato2, Ato3 or Ady2 variants. However, slow, non-exponential growth was observed for strains expressing *ATO2*^{T653C} or any variant of *ADY2* which could indicate a minor change in affinity for this substrate caused by the point mutations.

3.4 Protein modelling reveals mutations in the central hydrophobic constriction site as important factor in determining substrate specificity

In order to establish a link between the observed phenotypes and the structural alterations of transporters carrying the mutated amino acid residues, the 3D protein structures of Ady2, Ato2 and Ato3 were predicted based on the crystal structure of the *Citrobacter koseri* acetate anion channel SatP (PDB 5YS3), a bacterial member of the AceTr family (Qui et al., 2018). When combined with a sequence alignment of Ady2, Ato2 and Ato3, the 3D structures showed that the Leu219Val mutation in Ady2, the Leu218Ser mutation in Ato2 and the Phe95Ser mutation in Ato3 are amongst three amino acid residues that were previously identified to be essential for the formation of the central narrowest hydrophobic constriction of the anion pathway in *C. koseri* SatP (Qui et al., 2018) (Figure 3 and Figure 4). Specifically, these changes result in the substitution of the amino acid side group with a smaller (and in the case of Ato2 and Ato3 a more hydrophilic) alternative (Ato3 is shown in Figure 4 and the models for Ady2 and Ato2 can be found in Supplementary Figures 9 and 10). Based on these models, we estimated the distance between these three hydrophobic residues. Since these distances are based on model predictions and are, for instance, dependent on the rotation of the amino acid side chains, they should not be interpreted as exact values. However, when comparing the relative distances, we found an increased value for *ADY2*^{C655G}, *ATO3*^{T284C} and *ATO2*^{T653C} compared to

403 their corresponding wildtype protein, leading to a larger aperture in the center of the channel
404 (Table 4). We hypothesize that this increased size of the hydrophobic constriction may allow
405 larger substrates to pass through, possibly altering substrate specificity and transport
406 capacity.
407 To investigate if the mutations affected the presence and affinity of binding sites for acetate,
408 lactate and pyruvate, docking of ligands in the protein structures was simulated using
409 AutoDock Vina (Supplementary Figure 10, Supplementary Table 2). In all proteins, both
410 wildtype and mutated, four binding sites were identified for acetate, which is in accordance
411 with what has previously been reported for the homolog CkSatP (Qui et al., 2018). Of these
412 four binding sites, two, which are located closest to the hydrophobic constriction, also
413 consistently bind lactate and pyruvate. Strikingly, mutations in Ady2, Ato2 and Ato3 led to an
414 increased lactate affinity of at least one of these two sites closest to the hydrophobic
415 constriction, which might have contributed to the increased lactate transport capacity. No
416 clear correlation was found between the physiology observed for strains overexpressing the
417 different protein variants when grown on acetate and pyruvate and the corresponding binding
418 affinities of these two ligands (Supplementary Table 2).
419

Figure 3: Multiple sequence alignment of *Citrobacter koseri* SatP and *Saccharomyces cerevisiae* Ady2, Ato2 and Ato3. The multiple sequence alignment was built with ClustalOmega (https://www.ebi.ac.uk/Tools/msa/clustalo/). Localization of transmembrane segments (TMSs) was predicted with PSI/TM-Coffee (http://tcoffee.crg.cat/apps/tcoffee/do:tmcoffee). Blue rectangles indicate residues of the narrowest constriction site F98-Y155-L219 (amino acid numbers refer to Ady2) (Qui et al., 2018). Bold, underlined letters indicate the mutated residue.

Table 4: Estimated average distances (in Å) between different amino acids (AA) in the constriction pore of Ady2, Ato2 Ato3 and mutated alleles, calculated using the corresponding protein model. Bold values in the table indicate distances which are at least 1 Å larger than calculated in the reference structure.

Protein	Estimated distance between AA residues			Protein	Estimated distance between AA residues			Protein	Estimated distance between AA residues		
	219&98	98&155	155&219		218&97	97&154	154&218		215&95	95&152	152&215
Ady2	4.6	6.9	4.0	Ato2	4.2	5.7	4.4	Ato3	4.0	4.6	4.1
Ady2 L219V	4.4	6.9	**5.3**	Ato2 L218S	**5.9**	5.6	**5.6**	Ato3 F95S	**7.7**	**8.5**	4.5
Ady2 A252G	4.5	6.7	3.9								

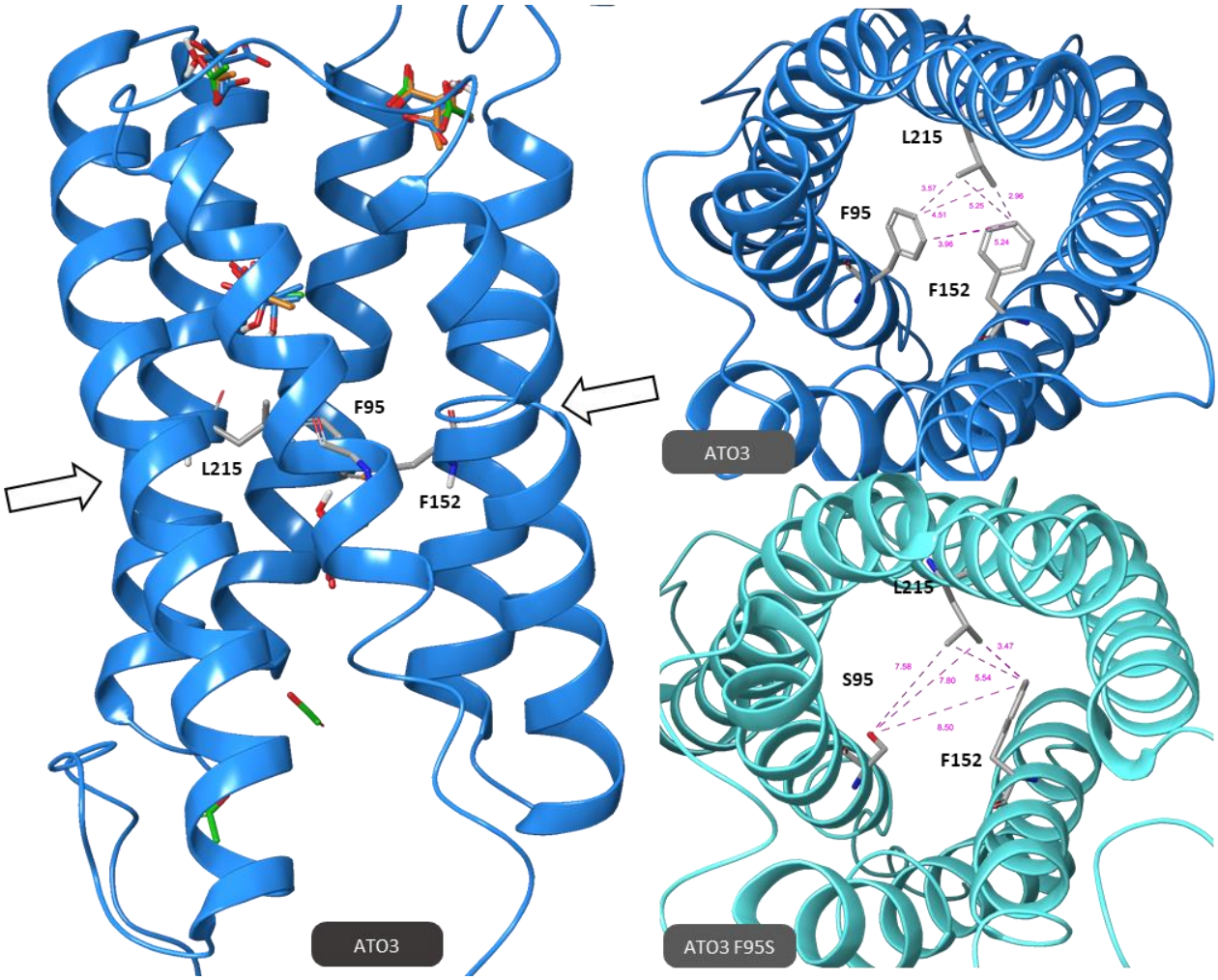

Figure 4: 3D models of the transporters Ato3 (dark blue) and Ato3^{F95S} (light blue). Left: side view of Ato3. Arrows indicate the hydrophobic constriction site, consisting of F95, L215 and F152. Binding sites for acetate (green ligand), lactate (blue ligand) and pyruvate (orange ligand) are presented. Right, top view of Ato3 (top) and Ato3^{F95S}(bottom). The amino acids involved in the constriction site are shown. Purple lines and values indicate estimated distances (in Å) between different anchor points of amino acids, calculated from the modelled protein structure.

4. DISCUSSION

In this study, we report the identification and characterization of a family of transporter genes which, upon mutation, are able to efficiently catalyze the import of lactic acid in *S. cerevisiae*. As rational engineering to identify lactic acid transporters remains elusive (Borodina, 2019; Mans et al., 2017), we used adaptive laboratory evolution to select for mutants capable of consuming lactic acid, which led to the identification of mutations in *ATO3* (*ATO3*^{T284C}) and *ATO2* (*ATO2*^{T653C}). Together with *ADY2*, *ATO2* and *ATO3* were previously described to code for ammonium transporters (Ammonium Transport Outwards) based on two observations: the high expression levels of these genes when *S. cerevisiae* exports ammonium, and the presence of a motif associated with ammonium transport in the encoded proteins (Palková et al., 2002). However, the function of *ADY2* has previously been assessed by (Rabitsch et al., 2001), who identified it as a gene required for correct spore formation, and thus named it as *ADY2* (Accumulation of DYads). In view of the observations in our study, where *ADY2*, *ATO2* and *ATO3* and their evolved variants catalyzed uptake of lactic and in some cases acetic acid, and the absence of mechanistic studies aimed at illustrating the phenomenon of ammonium export, we support the recent proposition by (Alves et al., 2020) to rename these genes, present in *S. cerevisiae* and other yeasts, as "Acetate Transporter Ortholog".

For physiological studies focused on organic acid substrate uptake, a platform strain devoid of organic acid importers is a useful tool as it enables characterization based on growth rate. No growth was observed for IMC164 (25 deletions and empty vector) on medium containing either lactic acid or pyruvate as sole carbon source (Figure 1), demonstrating that this is a suitable strain background to test pyruvic and lactic acid transport capacity of transporter variants. Strain IMK982 (*jen1Δ ady2Δ ato3Δ ato2Δ)* was also unable to grow on lactic acid, nor

could it evolve this trait, which suggests that this strain could also be employed as a platform strain to investigate both endogenous and heterologous lactic acid transporters, without requiring the additional 21 deletions. In contrast, when grown on acetic acid at pH 6.0, IMC164 exhibited non-exponential linear growth (Supplementary Figure 6), suggesting simple diffusion of acetic acid, or the presence of at least one gene involved in acetate transport in this strain background. The observed increase in the uptake rate of acetic acid for the evolved Ady2 and Ato2 variants (Figure 2) corroborates with the increased growth rate on this carbon source. For the strain expressing native *ATO3* an improved growth rate was observed, but no increase in acetic acid uptake could be detected. This result led us to postulate the role of Ato3 as an exporter of acetic acid, thereby limiting the negative effects caused by the passive diffusion of this monocarboxylic acid. The fact that the expression of native *ATO3*, besides *ADY2*, results in an increased growth rate on acetate is in accordance with previous data reporting that both genes are induced in cells shifted from glucose to acetic acid as sole carbon source (Paiva et al., 2004).

It was reported by de Kok et al., (2012) that the overexpression of *ADY2*, under the control of the strong glycolytic promoter *TEF1*, was sufficient to enable slow growth (μ_{max} ~0.02 h^{-1}) in medium containing lactic acid as sole carbon source. While the native alleles of *ATO3* and likely *ATO2* were not able to sustain growth on lactic acid medium, their mutated versions (*ATO2*^{T653C} and *ATO3*^{T284C}) enabled high growth rates, with the highest growth rate determined at 0.15 ± 0.01 h^{-1} for the strain harboring *ATO3*^{T284C}. To the best of our knowledge this growth rate represents the highest reported growth rate of *S. cerevisiae* expressing a single transport protein on lactic acid and is close to the growth rate observed by de Kok et al., (2012) of 0.14 h^{-1} by a strain expressing *ADY2*^{C655G}. This 3-fold increase in growth rate of the engineered strain compared to the reference strain CEN.PK113-7D indicates that, in non-engineered *S.*

493 *cerevisiae* strains, growth on lactic acid is likely limited by its transport into the cell, and not
494 the capacity to be further metabolized. Therefore, for future work that requires fast
495 consumption of lactic acid, overexpression of $ATO3^{T284C}$ can be considered.

496 Based on the 3D structures of Ady2 (Ato1), Ato2 and Ato3 and the simulation of ligand docking
497 in the predicted protein structures, we postulate that an increased binding affinity upon
498 mutation may contribute to increased transport capacity by facilitating passage of the ligand
499 through the hydrophobic constriction, although the increased size of the hydrophobic
500 constriction is probably the main contributor to the evolved phenotype. Other mechanisms
501 may also contribute to an improved transport capacity, as observed for the A252G mutation
502 in Ady2, an amino acid residue located outside the constriction pore. These may include an
503 improved transition between the closed to open state of the transporter or increased stability
504 in the plasma membrane.

505 In this study, we show that laboratory evolution is a powerful tool for the identification of
506 genes involved in substrate transport and resulted in the identification of $Ato3^{F95S}$, which
507 enables the highest growth rate on lactic acid by *S. cerevisiae* reported in strains expressing a
508 single transport protein thus far. In addition, the presented data on transporter structure and
509 function led to the identification of important amino acid residues that dictate substrate
510 specificity of *S. cerevisiae* carboxylic acid transporters, which could potentially aid in future
511 rational engineering and annotation of additional proteins involved in organic acid transport.

5. REFERENCES

Agrimi, G., Steiger, M. G., 2021. Metabolite transport and its impact on metabolic engineering approaches. FEMS Microbiology Letters. 368.

Alves, R., Sousa-Silva, M., Vieira, D., Soares, P., Chebaro, Y., Lorenz, M. C., Casal, M., Soares-Silva, I., Paiva, S., 2020. Carboxylic Acid Transporters in *Candida* Pathogenesis. mBio. 11.

Anjos, J., de Sousa, H. R., Roca, C., Cásio, F., Luttik, M. A., Pronk, J. T., Salema-Oom, M., Gonc¸alves, P., 2013. Fsy1, the sole hexose-proton transporter characterized in *Saccharomyces yeasts*, exhibits a variable fructose:H^+ stoichiometry. Biochimica et Biophysica Acta. 1828**,** 201-207.

Borodina, I., 2019. Understanding metabolite transport gives an upper hand in strain development. Microbial Biotechnology. 12**,** 69-70.

Botstein, D., Falco, S. C., Steward, S. E., Brennan, M., Scherer, S., Stinchcomb, D. T., Struhl, K., Davis, R. W., 1979. Sterile Host Yeasts (SHY): A Eukaryotic System of Biological Containment for Recombinant DNA Techniques. Gene. 8**,** 17-24.

Bueno, J. G. R., Borelli, G., Corrêa, T. L. R., Fiamenghi, M. B., José, J., de Carvalho, M., de Oliveira, L. C., Pereira, G. A. G., dos Santos, L. V., 2020. Novel xylose transporter Cs4130 expands the sugar uptake repertoire in recombinant *Saccharomyces cerevisiae* strains at high xylose concentrations. Biotechnology for Biofuels. 13.

Casal, M., Paiva, S., Andrade, R. P., Gancedo, C., Leão, C., 1999. The Lactate-Proton Symport of *Saccharomyces cerevisiae* Is Encoded by *JEN1*. Journal of Bacteriology. 181**,** 2620-2623.

Casal, M., Queirós, O., Talaia, G., Ribas, D., Paiva, S., 2016. Carboxylic Acids Plasma Membrane Transporters in Saccharomyces cerevisiae. In: Ramos, J., Sychrová, H., Kschischo, M., Eds.), Yeast Membrane Transport. Springer International Publishing, Cham, pp. 229-251.

Chattopadhyay, A., Singh, R., Das, A. K., Maiti, M. K., 2020. Characterization of two sugar transporters responsible for efficient xylose uptake in an oleaginous yeast *Candida tropicalis* SY005. Archives of Biochemistry and Biophysics. 695.

Cherry, J. M., Hong, E. L., Amundsen, C., Balakrishnan, R., Binkley, G., Chan, E. T., Christie, K. R., Costanzo, M. C., Dwight, S. S., Engel, S. R., Fisk, D. G., Hirschman, J. E., Hitz, B. C., Karra, K., Krieger, C. J., Miyasato, S. R., Nash, R. S., Park, J., Skrzypek, M. S., Simison, M., Weng, S., Wong, E. D., 2012. Saccharomyces Genome Database: the genomics resource of budding yeast. Nucleic Acids Research. 40**,** D700-D705.

Colabardini, A. C., Ries, L. N. A., Brown, N. A., dos Reis, T. F., Savoldi, M., Goldman, M. H. S., Menino, J. F., Rodrigues, F., Goldman, G. H., 2014. Functional characterization of a xylose transporter in *Aspergillus nidulans*. Biotechnology for Biofuels. 7.

de Kok, S., Nijkamp, J. F., Oud, B., Roque, F. C., de Ridder, D., Daran, J.-M. G., Pronk, J. T., van Maris, A. J. A., 2012. Laboratory evolution of new lactate transporter genes in a *jen1Δ* mutant of *Saccharomyces cerevisiae* and their identification as *ADY2* alleles by whole-genome resequencing and transcriptome analysis. FEMS Yeast Research. 12**,** 359-374.

Entian, K.-D., Kötter, P., 2007. Yeast Genetic Strain and Plasmid Collections. Methods in Microbiology. 36**,** 629-666.

Gabba, M., Frallicciardi, J., van 't Klooster, J., Henderson, R., Syga, L., Mans, R., van Maris, A. J. A., Poolman, B., 2020. Weak Acid Permeation in Synthetic Lipid Vesicles and Across the Yeast Plasma Membrane. Biophysical Journal. 118**,** 422-434.

Gao, M., Ploessl, D., Shao, Z., 2019. Enhancing the Co-utilization of Biomass-Derived Mixed Sugars by Yeasts. Frontiers in Microbiology. 9.

Gietz, R. D., Woods, R. A., 2002. Transformation of Yeast by Lithium Acetate/Single-Stranded Carrier DNA/Polyethylene Glycol Method. Methods in Enzymology. 350**,** 87-96.

Huang, W., Hu, B., Liu, J., Zhou, Y., Liu, S., 2020. Identification and Characterization of Tonoplast Sugar Transporter (TST) Gene Family in Cucumber. Horticultural Plant Journal. 6**,** 145–157.

Kruckeberg, A. L., Dickinson, J. R., 2004. Carbon Metabolism. In: Dickinson, J. R., Schweizer, M., Eds.), The metabolism and molecular physiology of *Saccharomyces cerevisiae*. Taylor & Francis Ltd, London, pp. 42-103.

Lagunas, R., 1993. Sugar transport in *Saccharomyces cerevisiae*. FEMS Microbiology Reviews. 104**,** 229-242.

Li, H., Durbin, R., 2010. Fast and accurate long-read alignment with Burrows–Wheeler transform. Bioinformatics. 26**,** 589-595.

Li, H., Handsaker, B., Wysoker, A., Fennell, T., Ruan, J., Homer, N., Marth, G., Abecasis, G., Durbin, R., Subgroup, G. P. D. P., 2009. The Sequence Alignment/Map format and SAMtools. Bioinformatics. 25**,** 2078-2079.

Li, H., Schmitz, O., Alper, H. S., 2016. Enabling glucose/xylose co-transport in yeast through the directed evolution of a sugar transporter. Applied Microbiology and Biotechnology. 100**,** 10215–10223.

Li, J., Xu, J., Cai, P., Wang, B., Ma, Y., Benz, J. P., Tian, C., 2015. Functional Analysis of Two L-Arabinose Transporters from Filamentous Fungi Reveals Promising Characteristics for Improved Pentose Utilization in *Saccharomyces cerevisiae*. Applied and Environmental Microbiology. 81**,** 4062–4070.

Mans, R., Daran, J.-M. G., Pronk, J. T., 2018. Under pressure: evolutionary engineering of yeast strains for improved performance in fuels and chemicals production. Current Opinion in Biotechnology. 50**,** 47-56.

Mans, R., Hassing, J.-E., Wijsman, M., Giezekamp, A., Pronk, J. T., Daran, J.-M. G., Van Maris, A. J. A., 2017. A CRISPR/Cas9-based exploration into the elusive mechanism for lactate export in *Saccharomyces cerevisiae*. FEMS Yeast Research. 17**,** 1-12.

Mans, R., van Rossum, H. M., Wijsman, M., Backx, A., Kuijpers, N., van den Broek, M., Daran-Lapujade, P., Pronk, J. T., van Maris, A. J. A., Daran, J.-M. G., 2015. CRISPR/Cas9: a molecular Swiss army knife for simulaneous introduction of multiple genetic modifications in *Saccharomyces cerevisiae*. FEMS Yeast Research. 15**,** 1-15.

Marques, W. L., Mans, R., Marella, E. R., Cordeiro, R. L., Van den Broek, M., Daran, J.-M. G., Pronk, J. T., Gombert, A. K., van Maris, A. J. A., 2017. Elimination of sucrose transport and hydrolysis in *Saccharomyces cerevisiae*: a platform strain for engineering sucrose metabolism. FEMS Yeast Research. 17**,** 1-11.

Morii, M., Sugihara, A., Takehara, S., Kanno, Y., Kawai, K., Hobo, T., Hattori, M., Yoshimura, H., Seo, M., Ueguchi-Tanaka, M., 2020. The Dual Function of OsSWEET3a as a Gibberellin and Glucose Transporter Is Important for Young Shoot Development in Rice. Plant Cell Physiology. 61**,** 1935–1945.

Mumberg, D., Müller, R., Funk, M., 1995. Yeast vectors for the controlled expression of heterologous proteins in different genetic backgrounds. Gene. 156**,** 119-122.

Nijland, J. G., Driessen, A. J. M., 2020. Engineering of Pentose Transport in *Saccharomyces cerevisiae* for Biotechnological Applications. Frontiers in Bioengineering and Biotechnology. 7.

Nogueira, K. M. V., Mendes, V., Carraro, C. B., Taveira, I. C., Oshiquiri, L. H., Gupta, V. K., Silva, R. N., 2020. Sugar transporters from industrial fungi: Key to improving second-generation ethanol production. Renewable and Sustainable Energy Reviews. 131.

Paiva, S., Devaux, F., Barbosa, S., Jacq, C., Casal, M., 2004. Ady2p is essential for the acetate permease activity in the yeast *Saccharomyces cerevisiae*. Yeast. 21**,** 201-210.

Palková, Z., Devaux, F., Řičicová, M., Mináriková, L., Le Crom, S., Jacq, C., 2002. Ammonia Pulses and Metabolic Oscillations Guide Yeast Colony Development. Molecular Biology of the Cell. 13**,** 3901–3914.

Paulsen, P. A., Custódio, T. F., Pedersen, B. P., 2019. Crystal structure of the plant symporter STP10 illuminates sugar uptake mechanism in monosaccharide transporter superfamily. Nature Communications. 10.

Pinheiro, C., Longatto-Filho, A., Azevedo-Silva, J., Casal, M., Schmitt, F., Baltazar, F., 2012. Role of monocarboxylate transporters in human cancers: state of the art. Journal of Bioenergetics and Biomembranes. 44**,** 127–139.

Pronk, J. T., 2002. Auxotrophic Yeast Strains in Fundamental and Applied Research. Applied and Environmental Microbiology. 68**,** 2095-2100.

Qui, B., Xia, B., Zhou, Q., Lu, Y., He, M., Hasegawa, K., Ma, Z., Zhang, F., Gu, L., Mao, Q., Wang, F., Zhao, S., Gao, Z., Liao, J., 2018. Succinate-acetate permease from *Citrobacter koseri* is an anion channel that unidirectionally translocates acetate. Cell Research. 28**,** 644–654.

Rabitsch, K. P., Tóth, A., Gálová, M., Schleiffer, A., Schaffner, G., Aigner, E., Rupp, C., Penkner, A. M., Moreno-Borchart, A. C., Primig, M., Esposito, R. E., Klein, F., Knop, M., Nasmyth, K., 2001. A screen for genes required for meiosis and spore formation based on whole-genome expression. Current Biology. 11**,** 1001-1009.

Ribas, D., Sá-Pessoa, J., Soarez-Silva, I., Paiva, S., Nygård, Y., Ruohonen, L., Penttilä, M., Casal, M., 2017. Yeast as a tool to express sugar acid transporters with biotechnological interest. FEMS Yeast Research. 17.

Ribas, D., Soares-Silva, I., Vieira, D., Sousa-Silva, M., Sá-Pessoa, J., Azevedo-Silva, J., Viegas, S. C., Arraiano, C. M., Diallinas, G., Paiva, S., Soares, P., Casal, M., 2019. The acetate uptake transporter family motif "NPAPLGL(M/S)" is essential for substrate uptake. Fungal Genetics and Biology. 122**,** 1-10.

Riesmeier, J. W., Willmitzer, L., Frommer, W. B., 1992. Isolation and characterization of a sucrose carrier cDNA from spinach by functional expression in yeast. The EMBO Journal. 11**,** 4705-4713.

Salazar, A. N., Gorter de Vries, A. R., van den Broek, M., Wijsman, M., de la Torre Cortéz, P., Brickwedde, A., Brouwers, N., Daran, J.-M. G., Abeel, T., 2017. Nanopore sequencing enables near-complete de novo assembly of *Saccharomyces cerevisiae* reference strain CEN.PK113-7D. FEMS Yeast Research. 17**,** 1-11.

Schmidl, S., Iancu, C. V., Reifenrath, M., Choe, J.-y., Oreb, M., 2021. A label-free real-time method for measuring glucose uptake kinetics in yeast. FEMS Yeast Research. 21.

Singhvi, M., Zendo, T., Sonomoto, K., 2018. Free lactic acid production under acidic conditions by lactic acid bacteria strains: challenges and future prospects. Applied Microbiology and Biotechnology. 102**,** 5911–5924.

Sloothaak, J., Tamayo-Ramos, J. A., Odoni, D. I., Laothanachareon, T., Derntl, C., Mach-Aigner, A. R., Martins dos Santos, V. A. P., Schaap, P. J., 2016. Identification and functional characterization of novel xylose transporters from the cell factories *Aspergillus niger* and *Trichoderma reesei*. Biotechnology for Biofuels. 9.

Soares-Silva, I., Ribas, D., Sousa-Silva, M., Azevedo-Silva, J., Rendulić, T., Casal, M., 2020. Membrane transporters in the bioproduction of organic acids: state of the art and future perspectives for industrial applications. FEMS Microbiology Letters. 367.

Sterling, T., Irwin, J. J., 2015. ZINC 15 − Ligand Discovery for Everyone. Journal of Chemical Information and Modeling. 55**,** 2324-2337.

Suzuki, Y., St Onge, R. P., Mani, R., King, O. D., Heilbut, A., Labunskyy, V. M., Chen, W., Pham, L., Zhang, L. V., Tong, A. H. Y., Nislow, C., Giaever, G., Gladyshev, V. N., Vidal, M., Schow, P., Lehár, J., Roth, F. P., 2011. Knocking out multigene redundancies via cycles of sexual assortment and fluorescence selection. Nature Methods. 8**,** 159–164.

Trott, O., Olson, A. J., 2010. AutoDock Vina: Improving the Speed and Accuracy of Docking with a New Scoring Function, Efficient Optimization, and Multithreading. 31**,** 455-461.

Verduyn, C., Postma, E., Scheffers, W. A., van Dijken, J. P., 1992. Effect of Benzoic Acid on Metabolic Fluxes in Yeasts: A Continuous-Culture Study on the Regulation of Respiration and Alcoholic Fermentation. Yeast. 8**,** 501-517.

Walker, B. J., Abeel, T., Shea, T., Priest, M., Abouelliel, A., Sakthikumar, S., Cuomo, C. A., Zeng, Q., Wortman, J., Young, S. K., Earl, A. M., 2014. Pilon: An Integrated Tool for Comprehensive Microbial Variant Detection and Genome Assembly Improvement. PLoS ONE. 9.

Wang, C., Shen, Y., Hou, J., Suo, F., Bao, X., 2013. An assay for functional xylose transporters in *Saccharomyces cerevisiae*. Analytical Biochemistry. 442**,** 241–248.
Wieczorke, R., Krampe, S., Weierstall, T., Kreidel, K., Hollenberg, C. P., Boles, E., 1999. Concurrent knock-out of at least 20 transporter genes is required to block uptake of hexoses in *Saccharomyces cerevisiae*. FEBS letters. 464**,** 123-128.
Zhang, W., Cao, Y., Gong, J., Bao, X., Chen, G., Liu, W., 2015. Identification of residues important for substrate uptake in a glucose transporter from the filamentous fungus *Trichoderma reesei*. Scientific Reports. 5.

6. Funding

This work was supported by the BE-Basic R&D Program, which was granted an FES subsidy from the Dutch Ministry of Economic Affairs, Agriculture and Innovation (EL&I); the strategic programme UID/BIA/04050/2019 funded by Portuguese funds through the FCT I.P.; the projects: PTDC/BIAMIC/5184/2014, funded by national funds through the Fundação para a Ciência e Tecnologia (FCT) I.P.; the European Regional Development Fund (ERDF) through the COMPETE 2020–Programa Operacional Competitividade e Internacionalização (POCI); EcoAgriFood: Innovative green products and processes to promote AgriFood BioEconomy [grant number NORTE-01–0145-FEDER-000009]; Norte Portugal Regional Operational Programme (NORTE 2020), under the PORTUGAL 2020 Partnership Agreement, through the European Regional Development Fund (ERDF); and UMINHO/BD/25/2016 PhD grant by the Norte2020 [grant number NORTE-08–5369-FSE-000060] and a FEBS Short-Term Fellowship to MSS.

SUPPLEMENTARY INFORMATION

Evolutionary engineering for lactic acid uptake reveals key amino acid residues involved in substrate specificity of *Saccharomyces cerevisiae* carboxylic acid transporters.

Nicolò Baldi[1]*, Sophie Claire de Valk[1]*, Maria Sousa-Silva[2,3], Margarida Casal[2,3], Isabel Soares-Silva[2,3] & Robert Mans[1]

[1]Department of Biotechnology, Delft University of Technology, Van der Maasweg 9, 2629HZ Delft, The Netherlands

[2]Centre of Molecular and Environmental Biology (CBMA), University of Minho, Campus de Gualtar, Braga, Portugal

[3]Institute of Science and Innovation for Bio-Sustainability (IB-S), University of Minho, Campus de Gualtar, Braga, Portugal

*Shared-first authorship

Corresponding author: Robert Mans, r.mans@tudelft.nl

Running title: Novel lactic acid transporters in yeast.

Supplementary Figure 1, 2, 3, 4, 5, 6, 7, 8, 9 and 10

Supplementary Table 1 and 2

22

23 *Supplementary Table 1: Primers used in this study*

Number	Name	Sequence (5’ -> 3’)	Purpose
8664	JEN1_targetRNA FW SspI	TGCGCATGTTTCGGCGTTCGAAACTTCTCCGCAGTGAAAGATAAATGATCGTCACTCAATATTAATTTACGTTTTAGAGCTAGAAATAGCAAGTTAAAATAAGGCTAGTCCGTTATCAAC	Construction of pUDR405
6262	CrRNA insert ADY2 fw	TGCGCATGTTTCGGCGTTCGAAACTTCTCCGCAGTGAAAGATAAATGATCCCCACCGTAAGAACATAATGGTTTTAGAGCTAGAAATAGCAAGTTAAAATAAGGCTAGTCCGTTATCAAC	Construction of pUDR405
6005	p426 CRISP rv	GATCATTTATCTTTCACTGCGGAGAAG	Construction of pUDR405 – pUDR420
8691	ATO3_targetRNA FW SspI	TGCGCATGTTTCGGCGTTCGAAACTTCTCCGCAGTGAAAGATAAATGATCGAGTATATCTCTTGAATATTGTTTTAGAGCTAGAAATAGCAAGTTAAAATAAG	Construction of pUDR420
13552	ATO3_targetRNA_RV_SspI	CTTATTTTAACTTGCTATTTCTAGCTCTAAAACAATATTCAAGAGATATACTCGATCATTTATCTTTCACTGCGGAGAAGTTTCGAACGCCGAAACATGCGCA	Construction of pUDR420
8688	ATO2_targetRNA FW Eco52I	TGCGCATGTTTCGGCGTTCGAAACTTCTCCGCAGTGAAAGATAAATGATCCGGCCGTCAAAAATTTTTAAGTTTTAGAGCTAGAAATAGCAAGTTAAAATAAG	Construction of pUDR767
6006	p426 CRISP fw	GTTTTAGAGCTAGAAATAGCAAGTTAAAATAAGGCTAGTC	Construction of pUDR420 and pUDR767

5921	Primer_pTEF1_rv	AAAACTTAGATTAGATTGCTATGCTTTCTTTCTAATGAGC	Linear p426-TEF backbone amplification
10547	p426-GPD backbone rv	TCATGTAATTAGTTATGTCACGC	Linear p426-TEF backbone amplification
13513	pTEF1_ATO3	TACAACTTTTTTTACTTCTTGCTCATTAGAAAGAAAGCATAGCAATCTAATCTAAGTTTTATGACATCGTCTGCTTCTTC	Construction of pUDE813 and pUDE814
13514	tCYC1_ATO3	CGGTTAGAGCGGATGTGGGGGGAGGGCGTGAATGTAAGCGTGACATAACTAATTACATGATTAAGGAGCATTTGGCATTG	Construction of pUDE813 and pUDE814
17168	pTEF1_ADY2_fw	TACAACTTTTTTTACTTCTTGCTCATTAGAAAGAAAGCATAGCAATCTAATCTAAGTTTTATGTCTGACAAGGAACAAACG	Construction of pUDE1002, pUDE1003 and pUDE1004
17169	tCYC1_ADY2_rv	CGGTTAGAGCGGATGTGGGGGGAGGGCGTGAATGTAAGCGTGACATAACTAATTACATGATTAAAAGATTACCCTTTCAGTAG	Construction of pUDE1002, pUDE1003 and pUDE1004
17170	pTEF1_JEN1_fw	TACAACTTTTTTTACTTCTTGCTCATTAGAAAGAAAGCATAGCAATCTAATCTAAGTTTTATGTCGTCGTCAATTACAGATG	Construction of pUDE1001
17171	tCYC1_JEN1_rv	CGGTTAGAGCGGATGTGGGGGGAGGGCGTGAATGTAAGCGTGACATAACTAATTACATGATTAAACGGTCTCAATATGCTCC	Construction of pUDE1001
17452	pTEF1_ATO2_fw	TACAACTTTTTTTACTTCTTGCTCATTAGAAAGAAAGCATAGCAATCTAATCTAAGTTTTATGTCTGACAGAGAACAAAGC	Construction of pUDE1021 and pUDE1022
17453	tCYC1_ATO2_rv	CGGTTAGAGCGGATGTGGGGGGAGGGCGTGAATGTAAGCGTGACATAACTAATTACATGATTAGAAGAACACCTTATCATTGC	Construction of pUDE1021 and pUDE1022
17742	p426_CENARS_fw	TAGAAAAATAAACAAATAGGGGTTCCGCGCACATTTCCCCGAAAAGTGCCACCTGAACGAACGGATCGCTTGCCTGTAAC	Amplification of CEN6 from pUDC156
17743	p426_CENARS_rv	GATAATATCACAGGAGGTACTAGACTACCTTTCATCCTACATAAATAGACGCATATAAGTTCCCCGAAAAGTGCCACCTG	Amplification of CEN6 from pUDC156

2949	F Tag Episomal Rev	CGTTCAGGTGGCACTTTTCG	Construction of pUDC319-pUDC327
17741	p426_origi nremoval	ACTTATATGCGTCTATTTATGTAGGATG	Construction of pUDC319-pUDC327
1742	LEU2 check fw	GGTCGCCTGACGCATATACC	*LEU2* amplification
1743	LEU2 check rv	TAAGGCCGTTTCTGACAGAG	*LEU2* amplification
1738	HIS3 check fw	GCAGGCAAGATAAACGAAGG	*HIS3* amplification
3755	his3 outside rv (B)	CACTTGTTCGCTCAGTTCAG	*HIS3* amplification
8597	JEN1_repai r oligo fw	AAGAAGAGTAACAGTTTCAAAAGTTTTTCCTCAAAGAGATTAA ATACTGCTACTGAAAATTCACTTTTCATTGCTCTCTAGGGCGTG TTCGCTTCTCTATGTAACTGCATTTCACATATA	Deletion of *JEN1*
8598	JEN1_repai r oligo rv	TATATGTGAAATGCAGTTACATAGAGAAGCGAACACGCCCTAG AGAGCAATGAAAAGTGAATTTTCAGTAGCAGTATTTAATCTCTT TGAGGAAAAACTTTTGAAACTGTTACTCTTCTT	Deletion of *JEN1*
8665	ADY2_repai r oligo fw	CGACAGCTAACACAGATATAACTAAACAACCACAAAACAACTC ATATACAAACAAATAATGAGCACGACCTACTAATAACGAGAAC TATTGAAATAAAAAAGAGTAGTTTTTTATTTTTC	Deletion of *ADY2*
8666	ADY2_repai r oligo rv	GAAAAATAAAAAACTACTCTTTTTTATTTCAATAGTTCTCGTTAT TAGTAGGTCGTGCTCATTATTTGTTTGTATATGAGTTGTTTTGT GGTTGTTTAGTTATATCTGTGTTAGCTGTCG	Deletion of *ADY2*

14120	ATO3_repair_syn_fw	ATTGAGACGCTCCCCCAGCAGGGTTCGATTGCAGGCGTTTCGCAGGGCAGTAGAATTTCACCTAGACGTGGCCTTCTTGATGTTGATGTGTACATTGAAGAGCACGTGGGGTTTGTTCT	Deletion of *ATO3*
14121	ATO3_repair_syn_fw	AGAACAAACCCCACGTGCTCTTCAATGTACACATCAACATCAAGAAGGCCACGTCTAGGTGAAATTCTACTGCCCTGCGAAACGCCTGCAATCGAACCCTGCTGGGGGAGCGTCTCAAT	Deletion of *ATO3*
8689	ATO2_repair oligo fw	TATGTAACATTCTACAGATCAATCAAAAACAATCTTCAATCACAGAAAAAAATAAAAGGCAAACACAAAAGTGCAGGCTAAAATAACTTTTACCCCTATTATATATTCTTATGATCCATT	Deletion of *ATO2*
8690	ATO2_repair oligo rv	AATGGATCATAAGAATATATAATAGGGGTAAAAGTTATTTTAGCCTGCACTTTTGTGTTTGCCTTTTATTTTTTTCTGTGATTGAAGATTGTTTTTGATTGATCTGTAGAATGTTACATA	Deletion of *ATO2*

24

25

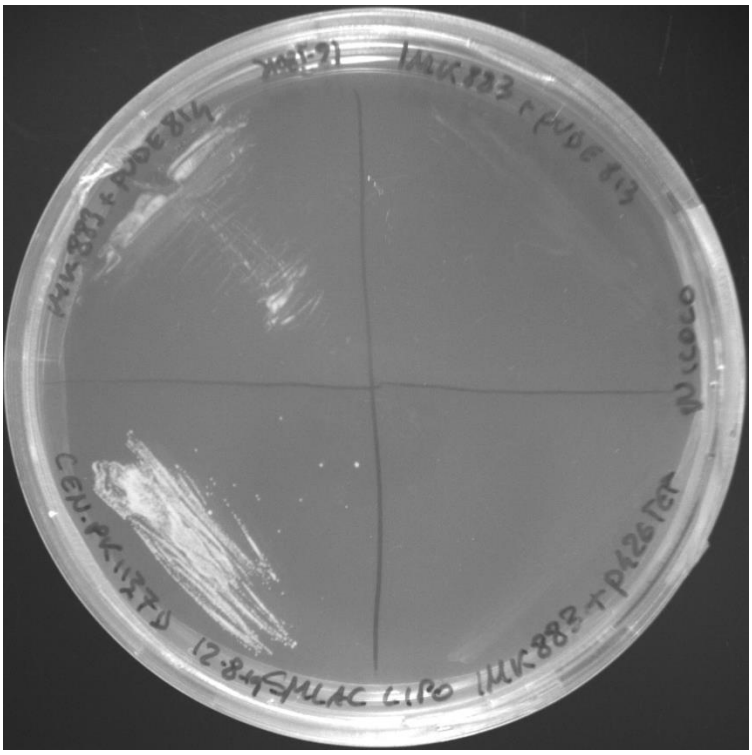

Supplementary Figure 1: Growth of different strains on SM media with lactic acid as the sole carbon source. Bottom left quadrant: prototrophic strain CEN.PK113-7D. Bottom right quadrant: IMK883 (ura3-52, jen1Δ, ady2Δ, ato3Δ) carrying an empty p426-pTEF plasmid. Top right quadrant: IMK883 carrying pUDE813 (p426-pTEF-ATO3). Top left quadrant: IMK883 carrying pUDE814 (p426-pTEF- $ATO3^{T284C}$). Cells were streaked from a single colony and the plate was incubated at 30 °C for 5 days.

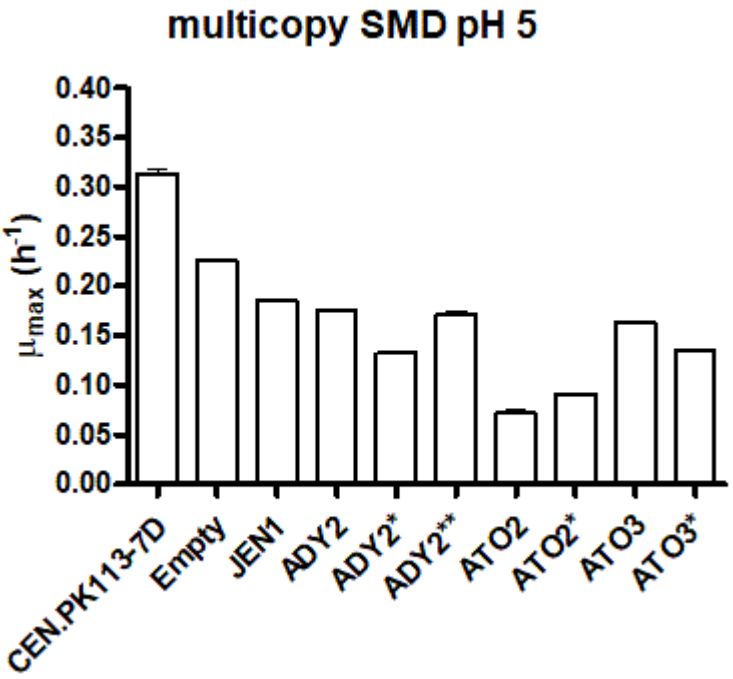

Supplementary Figure 2: Growth rates on SMD of *S. cerevisiae* reference strain CEN.PK113-7D and the 25-transporter deletion strain IMX2488 expressing an empty multicopy vector or a multicopy vector containing the indicated organic acid transporter gene. Bars and error bars represent the average and standard deviation of three independent experiments. Empty: empty plasmid. ADY2*: *ADY2*^{C755G} allele. ADY2**: *ADY2*^{C655G} allele. ATO2*: *ATO2*^{T653C} allele. ATO3*: *ATO3*^{T284C} allele.

33

34

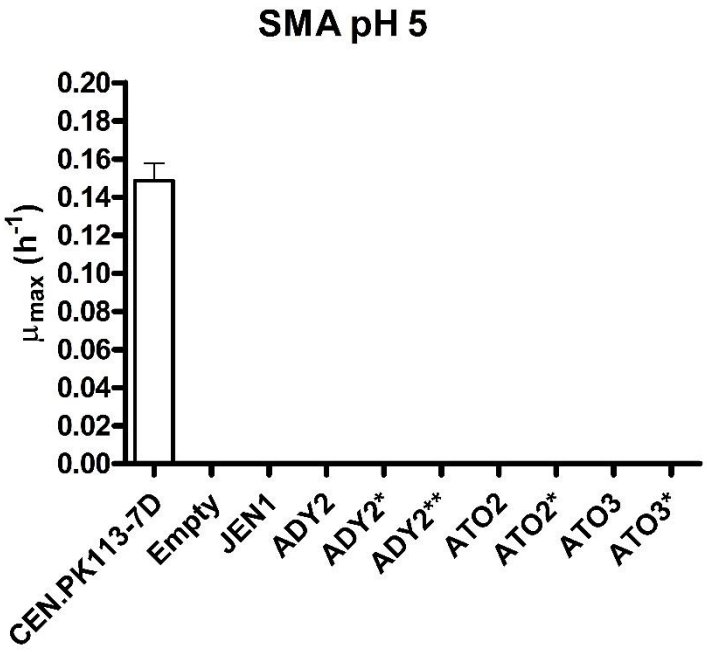

Supplementary Figure 3: Growth rates of *S. cerevisiae* reference strain CEN.PK113-7D and the 25-transporter deletion strain IMX2488 expressing an empty centromeric vector or a centromeric vectors containing the indicated organic acid transporter gene. Growth on SMA medium set at pH5. Bars and error bars represent the average and standard deviation of three independent experiments. Empty: empty plasmid. ADY2*: *ADY2*^{C755G} allele. ADY2**: *ADY2*^{C655G} allele. ATO2*: *ATO2*^{T653C} allele. ATO3*: *ATO3*^{T284C} allele.

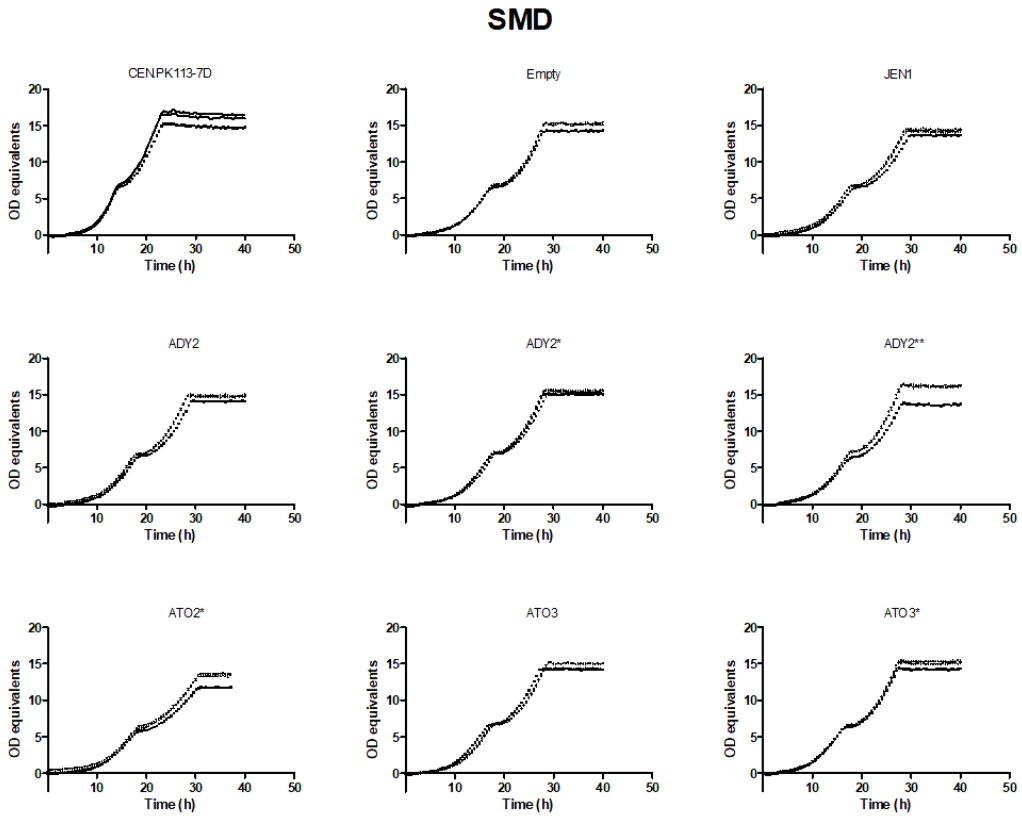

Supplementary Figure 4: Growth profiles in synthetic medium (pH 5.0) with glucose as the sole carbon source of CEN.PK113-7D and the 25-transporter deletion strain IMX2488 expressing an empty multicopy vector or a multicopy vector containing the indicated organic acid transporter gene. Empty: empty plasmid. ADY2*: *ADY2*^{C755G} allele. ADY2**: *ADY2*^{C655G} allele. ATO2*: *ATO2*^{T653C} allele. ATO3*: *ATO3*^{T284C} allele.

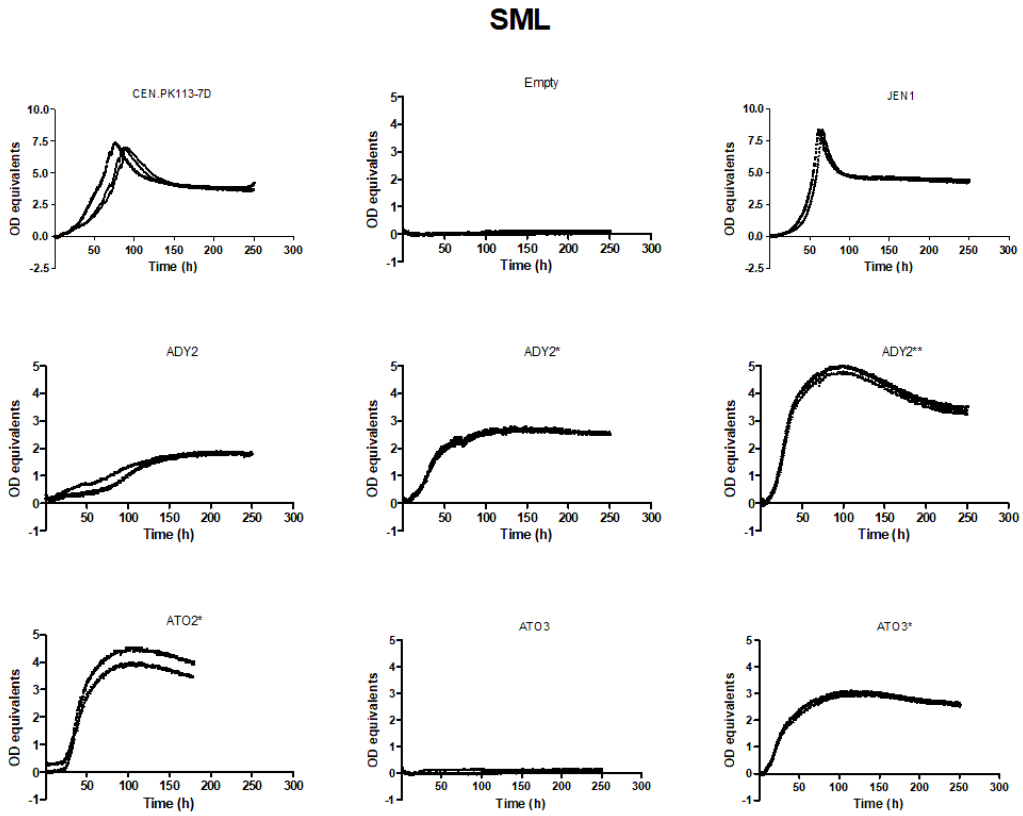

Supplementary Figure 5: Growth profiles in synthetic medium (pH 5.0) with lactate as the sole carbon source of CEN.PK113-7D and the 25-transporter deletion strain IMX2488 expressing an empty multicopy vector or a multicopy vector containing the indicated organic acid transporter gene. Empty: empty plasmid. ADY2*: *ADY2*^{C755G} allele. ADY2**: *ADY2*^{C655G} allele. ATO2*: *ATO2*^{T653C} allele. ATO3*: *ATO3*^{T284C} allele.

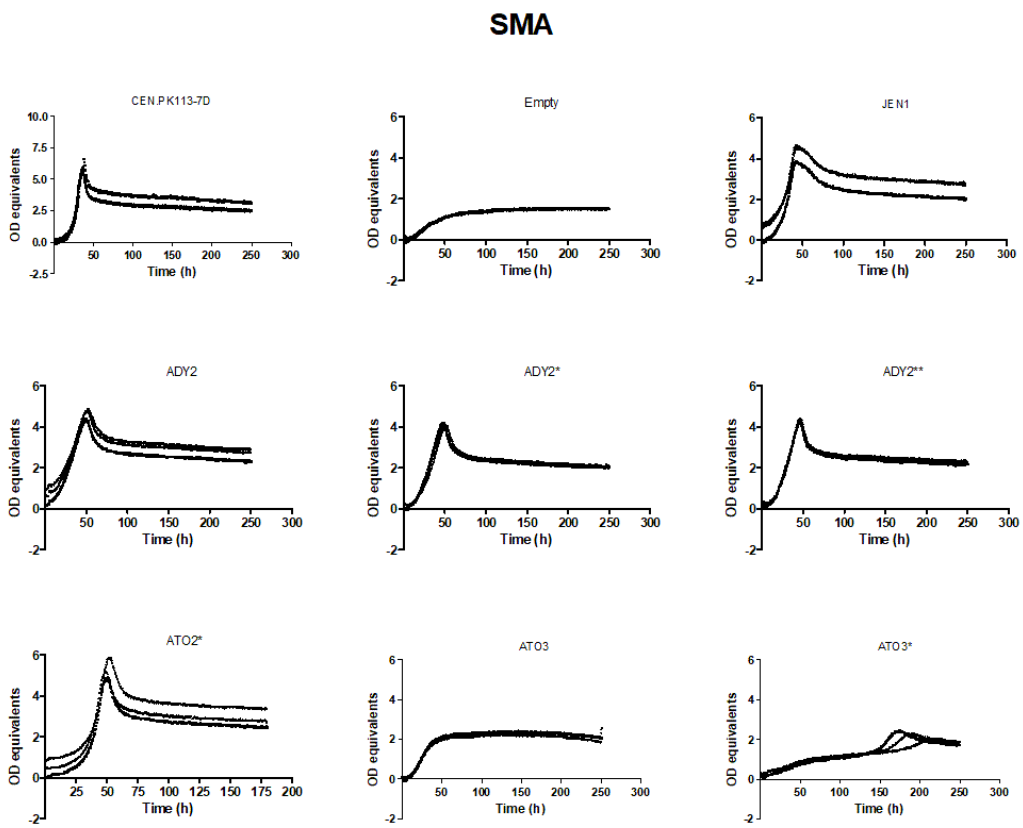

Supplementary Figure 6: Growth profiles in synthetic medium (pH 6.0) with acetate as the sole carbon source of CEN.PK113-7D and the 25-transporter deletion strain IMX2488 expressing an empty multicopy vector or a multicopy vector containing the indicated organic acid transporter gene. Empty: empty plasmid. ADY2*: *ADY2*^{C755G} allele. ADY2**: *ADY2*^{C655G} allele. ATO2*: *ATO2*^{T653C} allele. ATO3*: *ATO3*^{T284C} allele.

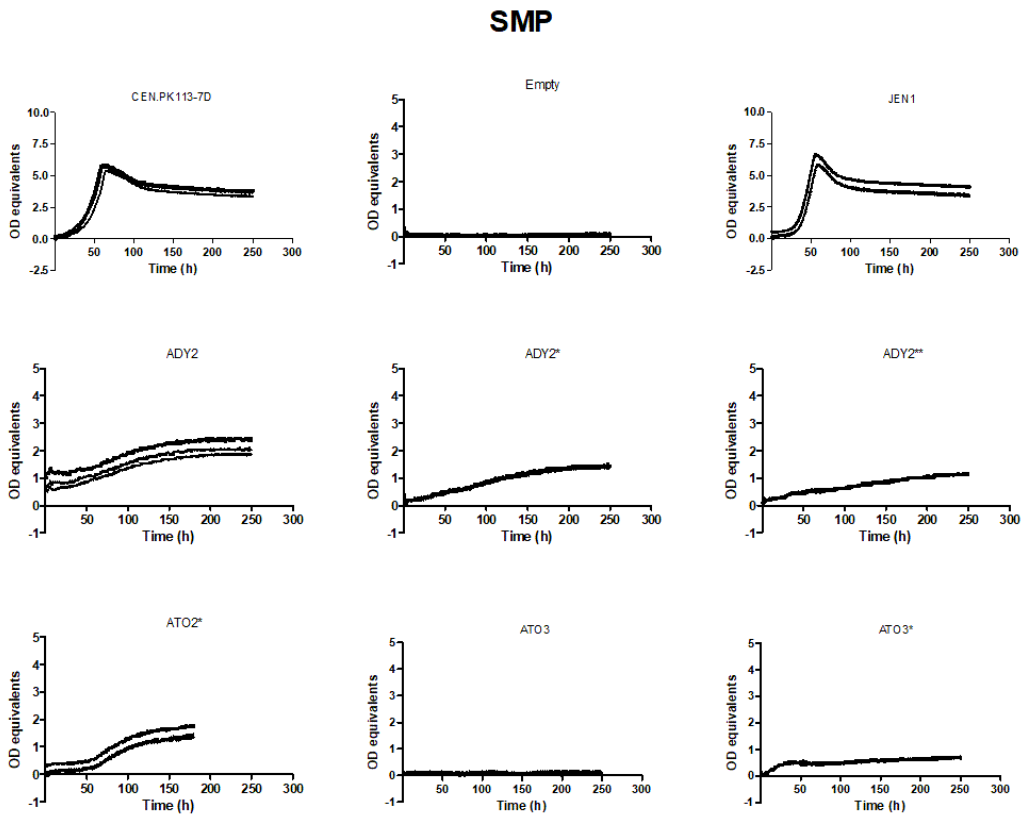

Supplementary Figure 7: Growth profiles in synthetic medium (pH 5) with pyruvate as the sole carbon source of CEN.PK113-7D and the 25-transporter deletion strain IMX2488 expressing an empty multicopy vector or a multicopy vector containing the indicated organic acid transporter gene. Empty: empty plasmid. ADY2*: *ADY2*^{C755G} allele. ADY2**: *ADY2*^{C655G} allele. ATO2*: *ATO2*^{T653C} allele. ATO3*: *ATO3*^{T284C} allele.

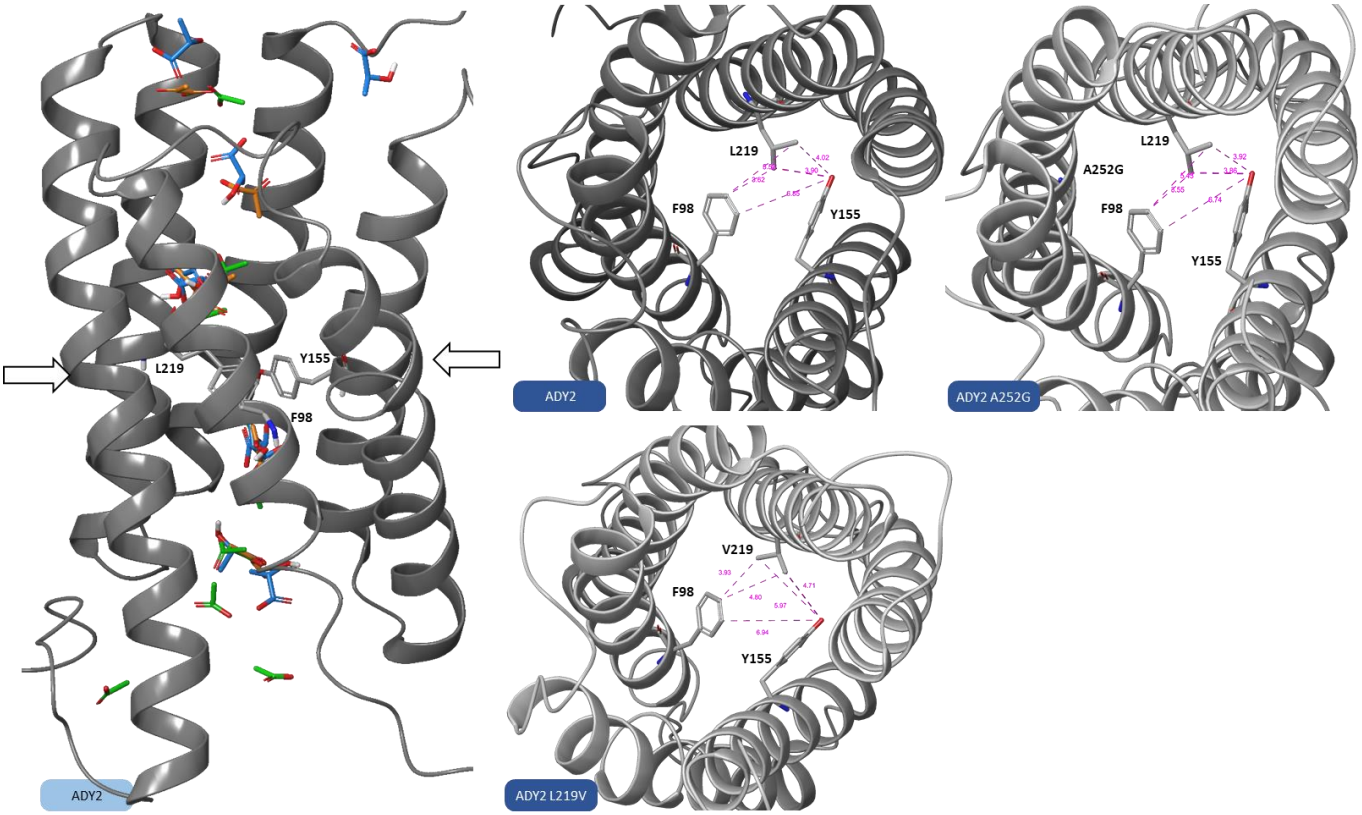

Supplementary Figure 8: 3D model of Ady2, Ady2^{C755G} and *Ady2*^{C655G} alleles*. Left, side view of Ady2. Arrows indicate the hydrophobic constriction site. Binding sites for acetate (green ligand), lactate (blue ligand) and pyruvate (orange ligand) are presented. Right, top view of Ady2, Ady2*^{C755G} and *Ady2*^{C655G} alleles*. The amino acids involved in the hydrophobic constriction site are shown. Purple lines and values indicate distances (in Å) between different anchor points of amino acids.*

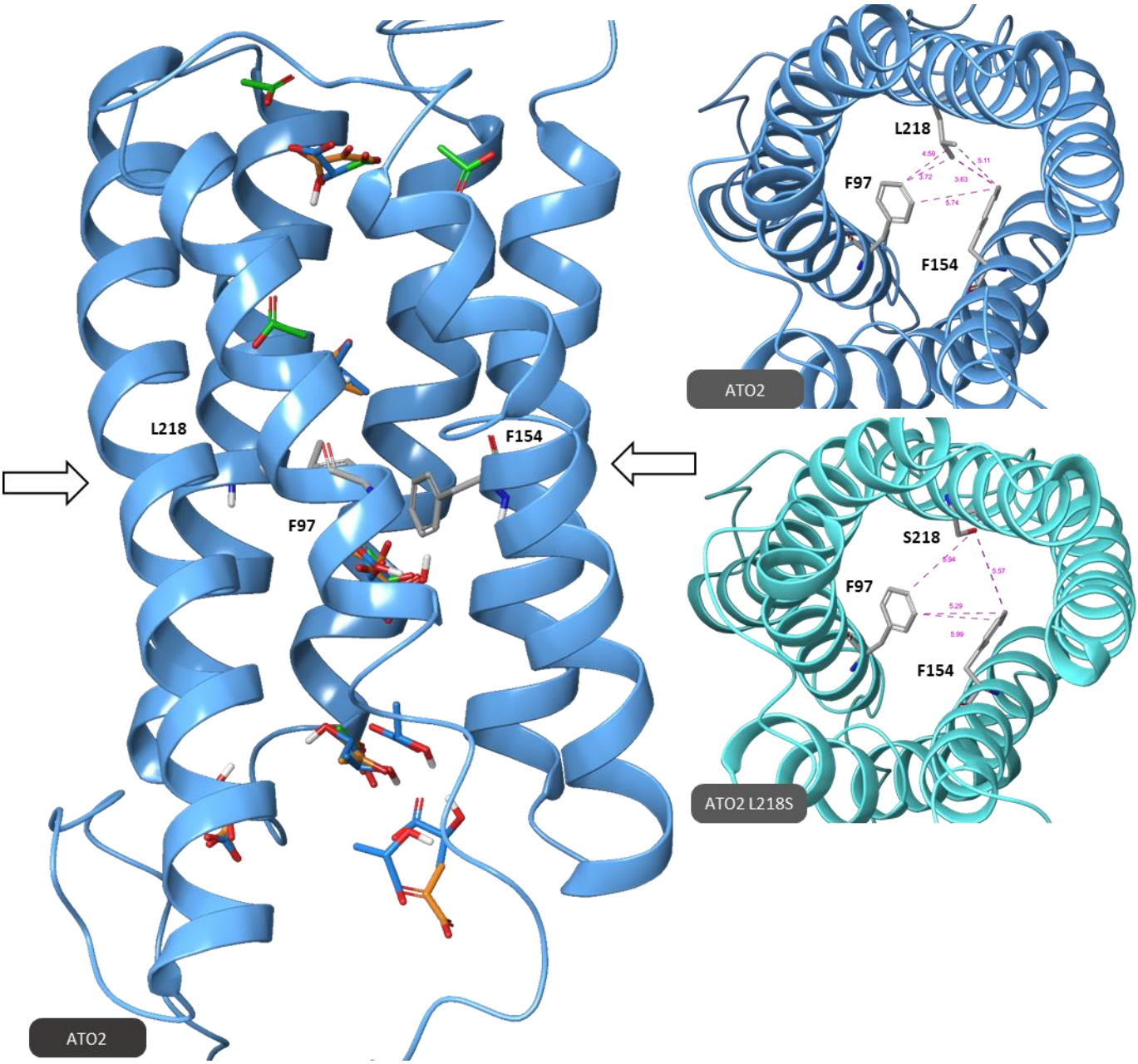

Supplementary Figure 9: 3D model of Ato2 and Ato2^{L218S}. Left, side view of Ato2. Arrows indicate the constriction site. Binding sites for acetate (green ligand), lactate (blue ligand) and pyruvate (orange ligand) are presented. Right, top view of either Ato2 or Ato2^{L218S}. The amino acids involved in the constriction site are shown. Purple lines and values indicate distances (in Å) between different anchor points of different amino acids.

Supplementary Table 2: Average of the binding affinity values [kcal/mol] calculated with PyRx software for the docking of ligand in the predicted structures of wildtype and mutated Ady2, Ato2 and Ato3.

3D-Protein templates	Average of binding affinities (kcal/mol) at different binding sites								
	Acetate								
	1			2	3	4			
	a	b	c			a	b	c	
Ady2	-2,1	-2,4	-2,3	-2,7	-3,1	-2,7	-	-	
Ady2 A252G	-2,3	-2,2	-2,1	-3,1	-3,1	-2,6	-2,7	-	
Ady2 L219V	-2,4	-	-	-3,0	-3,0	-2,5	-2,7	-	
Ato2	-2,5	-2,6	-	-3,1	-2,9	-2,8	-2,9	-3	
Ato2 L218S	-2,7	-	-	-2,7	-3,1	-3,3	-2,6	-2,5	
Ato3	-2,3	-2,2	-	-2,9	-3,0	-2,2	-	-2,4	
Ato3 F95S	-2,6	-2,4	-	-3,0	-2,9	-2,4	-2,4	-2,4	
	Lactate								
	1			2	3	4			
	a	b	c			a	b	c	d
Ady2	-	-3,1	-3,0	-3,6	-4,3	-3,5	-3,1	-3,1	-
Ady2 A252G	-2,9	-2,8	-2,7	-3,7	-4,4	-3,3	-3,4	-	-2,1
Ady2 L219V	-3,4	-	-	-3,9	-4,4	-	-3,8	-	-
Ato2	-3,2	-3,1	-3,2	-3,9	-3,8	-	-2,9	-	-
Ato2 L218S	-3,5	-	-	-3,8	-4,2	-3,6	-	-3,4	-
Ato3	-	-	-	-3,4	-3,8	-3,1	-	-3,2	-
Ato3 F95S	-3,3	-	-	-4,2	-4,0	-3,2	-3,2	-3,2	-
	Pyruvate								
	1			2	3	4			
	a	b	c			a	b	c	
Ady2	-	-3,1	-	-3,7	-4,2	-3,2	-3,3	-	
Ady2 A252G	-3,0	-	-2,7	-3,9	-4,3	-3,3	-3,3	-	
Ady2 L219V	-3,2	-	-	-4,0	-4,2	-	-3,5	-	
Ato2	-3,3	-3,3	-3,1	-3,9	-4,1	-	-3,6	-	
Ato2 L218S	-3,5	-	-	-3,9	-4,3	-	-	-3,3	
Ato3	-	-	-	-3,6	-4,0	-3,0	-	-3,2	
Ato3 F95S	-3,4	-	-	-4,2	-3,9	-	-3,4	-	

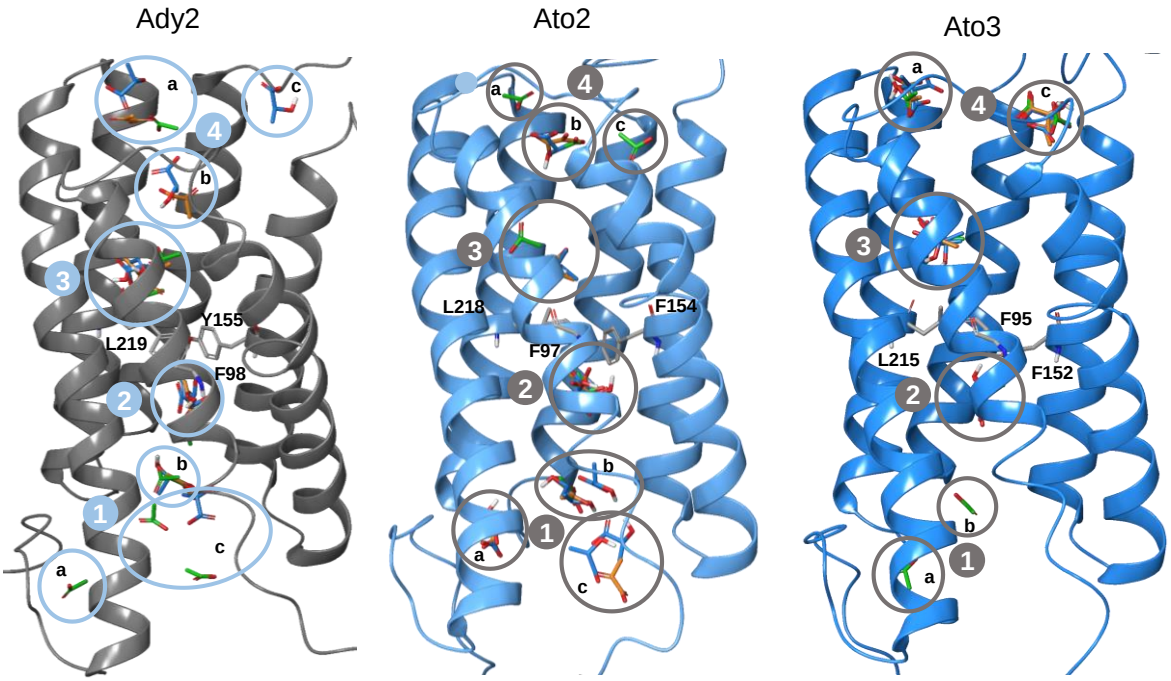

Supplementary Figure 10: Molecular docking sites of acetate (green ligand), lactate (blue ligand) and pyruvate (orange ligand) in the predicted structure of Ady2, Ato2 and Ato3, identified using Autodock Vina.